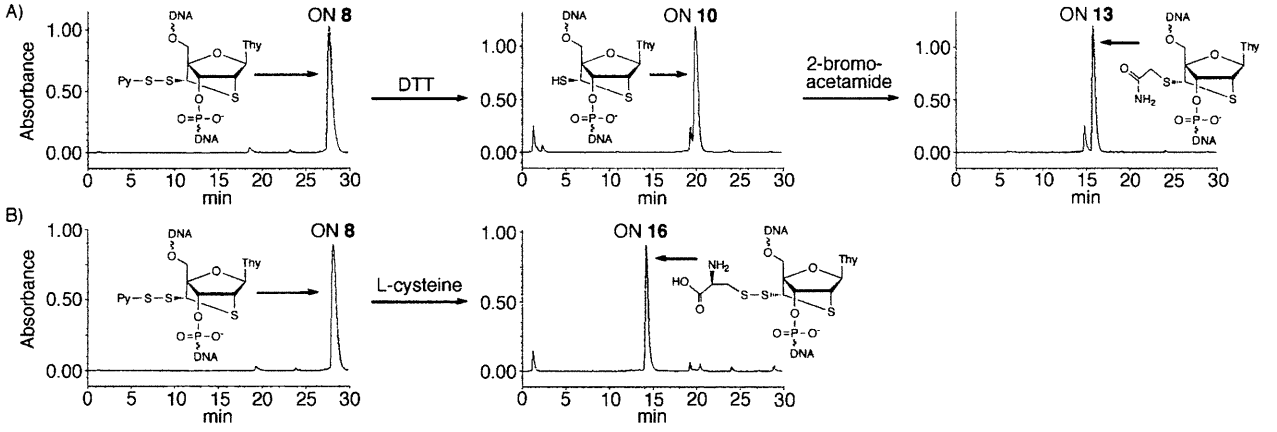

Fig. 3 RP-HPLC analyses of solution phase conjugations with a linear gradient of MeCN 6 to 12% over 30 min. (A) Thioether-linked conjugation with acetamide and (B) disulfide-linked conjugation with L-cysteine.

Evaluation of thermal stabilities

We evaluated the affinity of the synthesized ONs with complementary single-stranded RNA (ssRNA) and DNA (ssDNA) through UV melting experiments. The UV melting profiles are shown in Fig. S1 and S2 (ESI†), and the thermal denaturation temperatures (T_m values) are summarized in Table 1.

The T_m value of the ssDNA–ON **10** (containing naked thiol) duplex was lower than that of the natural DNA duplex (ΔT_m = −3 °C), but conjugation with a cationic group (ON **14**) led to improvement of the duplex stability (ΔT_m = −1 °C, $\Delta\Delta T_m$ = +2 °C). On the contrary, in the case of an anionic molecule conjugation, negative charge of carboxylic acid (ON **17**) destabilized its duplex with ssDNA (ΔT_m = −8 °C, $\Delta\Delta T_m$ = −5 °C). For the cationic group conjugate,[29] it reduced the electrostatic repulsion between the phosphodiester anions in contrast to the anionic group conjugate which increased it.[30] A pyrene conjugate also showed high duplex forming ability for ssDNA because of stacking effects or interaction between the pyrene moiety and hydrophobic nucleobases[31] (ΔT_m = +6 °C, $\Delta\Delta T_m$ = +9 °C). These data indicate that in DNA–DNA duplexes, conjugated groups and molecules directed toward the minor groove of duplexes and influence those hybridization properties.

ON **10** formed a stable duplex with complementary ssRNA (ΔT_m = +3 °C) in a similar manner to previous BNAs[3] because the bridged structure restricted the sugar conformation to N-type.[24] Surprisingly, in the DNA–RNA hybrid duplex, almost all conjugated molecules had no effect on the hybridization properties ($\Delta\Delta T_m$ = 0 °C to −1 °C) unlike double stranded DNA. This suggests that attached molecules are directed toward the outside of the helix in DNA–RNA hybrid duplexes and locked the positions by the rigid sugar conformation. The results have exhibited that, using this BNA, a wide variety of functional molecules can be attached to the center of the sequence, not 5′- or 3′-termini, without taking into account the affinity for target RNA. Generally, this characteristic is advantageous for antisense delivery technology.

Table 1 Evaluation of thermal denaturation temperatures (T_m values)

	DNA complement			RNA complement		
ON	T_m	ΔT_m[a]	$\Delta\Delta T_m$[b]/°C	T_m	ΔT_m[a]	$\Delta\Delta T_m$[b]/°C
natural	51	—	—	47	—	—
10	48[c]	−3	—	50[c]	+3	—
12	47	−4	−1	50	+3	0
13	48	−3	0	50	+3	0
14	50	−1	+2	49	+2	−1
15	57	+6	+9	47	0	−3
16	47	−4	−1	49	+2	−1
17	43	−8	−5	49	+2	−1

Each strand sequence: 5′-GCGTTXTTTGCT-3′ (X = modified monomer), target strand sequence: 5′-AGCAAAAAACGC-3′. Thermal denaturation studies' conditions: 10 mM sodium phosphate buffer (pH 7.2) containing 100 mM NaCl; each strand concentration = 4 μM; scan rate of 0.5 °C min^{-1} at 260 nm. The number is the average of three independent measurements.[a] ΔT_ms are calculated relative to T_m values of unmodified DNA–DNA and DNA–RNA duplexes. [b] $\Delta\Delta T_m$s are calculated relative to T_m values of ON **10**–DNA and ON **10**–RNA duplexes. [c] Thermal denaturation study's condition: 10 mM sodium phosphate buffer (pH = 7.4) containing 100 mM NaCl and 400 μM TCEP; each strand concentration = 4 μM; scan rate of 0.5 °C min^{-1} at 260 nm.

Effect of functional groups on nuclease resistances

We examined the resistance of decathymidilate derivatives involving a single thiol-containing BNA structure or its conjugates toward 3′-exonuclease (*Crotalus Adamanteus* Venom Phosphodiesterase, CAVP)[32] degradation and compared those with natural ssDNA and a phosphorothioate-modified ON (S-oligo). After incubation of each ON solution at 37 °C in the presence of CAVP, the ratio of intact ONs was analyzed at several time points by RP-HPLC (Fig. 4). The natural ssDNA was completely digested within 2 min, whereas ON **11** bearing a free thiol and its conjugates were considerably stable under these conditions; 90% of intact ON **11** survived after 40 min. In the same manner as other BNAs, 3′-phosphodiester linkages of these BNAs were hardly digested by the 3′-exonuclease, probably due to the sterically hindered environment around the 3′-phosphodiester linkage.[25] Although the nuclease resistance of natural DNA was the same either in the presence or absence of DTT (0.75 mM) and DTDP (3.8 μM), the reducing agent could not be excluded as the cause of the high enzymatic stability of ON **11** (free thiol).[32] Conjugation of some functional groups significantly enhanced the stability: acetamide-conjugate (ON **21**) and ethylamine-conjugate (ON **22**) were more stable than phosphorothioate-modified ON. This result is opposed

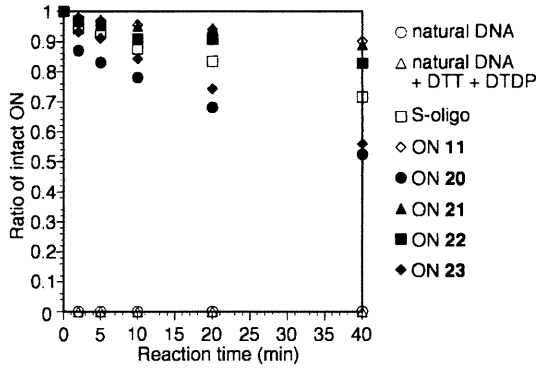

Fig. 4 Nuclease resistance of ONs against *Crotalus Adamanteus* Venom Phosphodiesterase (CAVP). Hydrolysis of the ONs (7.5 μM) was carried out at 37 °C in buffer (100 μL) containing 50 mM Tris-HCl (pH 8.5), 10 mM $MgCl_2$, and CAVP (0.35 μg). ON **11** was prepared by treating ON **9** with DTT and used without any purification.

to Chattopadhyaya's work;[33] introduction of amide or amine substitution lead to lowered enzymatic stability. Even though ON **20** (–Me) and ON **23** (–S-cationic tripeptide) were more degraded than ON **11**, these ONs were significantly more stable than natural ON. Since the enzymatic stabilities were not reflected in bulkiness of the ON conjugates, these results are attributed to other effects, not only to the steric effect.[34] However, the conjugation effects regarding the resistance to enzymatic degradation are not clear yet. We will soon elucidate the relevance between substituents at the C6′ position and nuclease resistances.

Response of disulfide linkage to glutathione

In order to make the best use of the disulfide linkage, it is necessary that the disulfide bond is cleaved. It is known that the disulfide bond is cleaved under intracellular reductive conditions.[12] But, it is possible that the disulfide bond is not cleaved because of the sterically hindered environment around the linkage. Thus, we assessed the response of the disulfide linkage in ON **18** to glutathione. Fig. 5 shows the RP-HPLC profile of conversion from ON **18** (disulfide form) to ON **10** (free thiol form). When treating ON **18** with glutathione (1 mM to 10 mM) for 30 min, the peak corresponding to ON **18** disappeared, and ON **10** was generated. This result demonstrates that the disulfide-linked conjugates will be cleaved on intracellular reductive conditions and the ONs with free thiol-containing BNA monomers be released in cells.

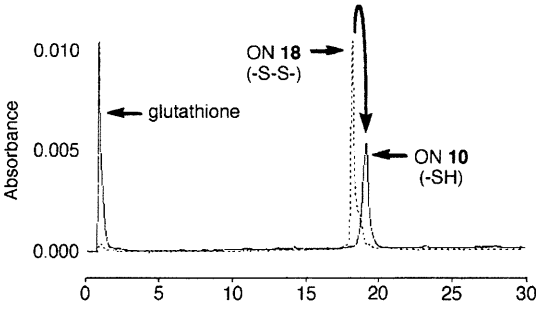

Fig. 5 RP-HPLC analysis of conversion from ON **18** to ON **10**. ON **18** in the absence of glutathione (dashed line) and in the presence of 10 mM glutathione (solid line).

Conclusions

We successfully synthesized a novel BNA bearing a thiol group in its bridged structure and conjugated functional molecules to it at the 6′-thiol group post-synthetically and efficiently in solution phase. Conjugated functional molecules had great effects on duplex stability with the DNA complement. In contrast, the molecules did not influence the stability with the RNA complement so much. Moreover, the ONs have as high or higher resistances against 3′-exonuclease than phosphorothioate ON (S-oligo).

Thus, this thiol-containing BNA is expected to have a wide field of application, for example, ON labeling, DNA detection, RNA-directed therapeutics, and DDS.

Experimental section

General

Dichloromethane, DMF and pyridine were distilled from CaH_2. ^1H NMR (400 and 300 MHz), ^{13}C NMR (100.5 and 75.5 MHz) and ^{31}P NMR (161.8 MHz) were recorded on JEOL JNM-ECS-400 or JNM-AL-300 spectrometers. Chemical shifts are reported in parts per million referenced to internal tetramethylsilane (0.00 ppm) and residual $CHCl_3$ (7.26 ppm) and methanol (3.31 ppm) for ^1H NMR, and chloroform-d_1 (77.0 ppm) and methanol-d_4 (49.0 ppm) for ^{13}C NMR. Relative to 85% H_3PO_4 as external standard for ^{31}P NMR. IR spectra were recorded on a JASCO FT/IR-4200 spectrometers. Optical rotations were recorded on a JASCO DIP-370 instrument. Mass spectra were measured on JEOL JMS-700 mass spectrometers. MALDI-TOF mass spectra were recorded on a Bruker Daltonics Autoflex II TOF/TOF mass spectrometer. For column chromatography, Fuji Silysia PSQ-100B or FL-100D silica gel was used. For high performance liquid chromatography (HPLC), SHIMADZU LC-6AD, SPD-10AV_{VP} and CTO-10A_{VP} were used.

1-{2-Thio-3,5-di-*O*-(*tert*-butyldiphenylsilyl)-2-*S*,4-*C*-(1-thiaethylene)-β-D-ribofuranosyl}thymine (2). To a solution of compound **1**[22] (50 mg, 0.16 mmol) and *N*,*N*-dimethyl-4-aminopyridine (96 mg, 0.79 mmol) in DMF (0.20 mL) was added *tert*-butyldiphenylsilyl chloride (0.14 mL, 0.55 mmol) and the resultant mixture was stirred at 100 °C for 15 h under a N_2 atmosphere. After addition of CH_3OH, the reaction mixture was diluted with Et_2O, washed with H_2O, dried over $MgSO_4$, and concentrated. The crude product was purified by column chromatography (n-hexane/AcOEt = 3/1) to give compound **2** (88 mg, 70%) as a white foam; $[\alpha]_D^{25}$ –21.2 (*c* 1.0, CH_2Cl_2); IR ν_{max} (KBr): 1690 cm^{-1}; ^1H NMR (300 MHz, $CDCl_3$) δ 1.00 (9 H, s), 1.10 (9 H, s), 1.43 (3 H, s), 2.77 (1 H, d, J = 13 Hz), 2.81 (1 H, d, J = 6 Hz), 3.38 (1 H, d, J = 12 Hz), 3.60 (1 H, d, J = 13 Hz), 3.71 (1 H, d, J = 12 Hz), 3.89 (1 H, d, J = 6 Hz), 6.58 (1 H, s), 6.77 (1 H, s), 7.16–7.63 (20 H, m), 7.98 (1 H, brs); ^{13}C NMR (75.5 MHz, $CDCl_3$) δ 12.2, 19.3, 19.3, 26.8, 27.0, 31.6, 51.6, 66.7, 68.3, 84.9, 89.2, 110.2, 127.8, 127.8, 127.9, 130.0, 130.2, 130.4, 132.2, 132.3, 132.6, 134.4, 135.4, 135.4, 135.6, 135.8, 149.6, 163.6; MS (FAB) *m/z* 795 (M + H^+); HRMS (FAB): Calcd for $C_{43}H_{51}N_2O_5S_2Si_2$ (M + H^+): 795.2778. Found: 795.2782.

1-[2-Thio-3,5-di-*O*-(*tert*-butyldiphenylsilyl)-2-*S*,4-*C*-{(*S*)-sulfanylmethylene}-β-D-ribofuranosyl]thymine (3). Compound **2** (200 mg, 0.25 mmol) was dissolved in CH_2Cl_2 (100 mL) at room temperature. The solution was stirred and photoirradiated by a high pressure mercury lamp at ambient temperature for 30 min. The solvent was removed to give compound **3** as a white foam. The product was used without purification; $[\alpha]_D^{25}$ +21.2 (*c* 1.0, CH_2Cl_2); IR ν_{max} (KBr): 1589, 1686, 1898, 1961, 2857, 2930, 3071, 3178 cm^{-1}; ^1H NMR (400 MHz, $CDCl_3$) δ 1.08–1.12 (21 H, m), 2.23 (1 H, d, J = 12 Hz), 3.01 (1 H, d, J = 2 Hz), 4.02 (1 H, d, J = 11 Hz), 4.45 (1 H, d, J = 12 Hz), 4.48 (1 H, d, J = 2 Hz), 4.57 (1 H, d, J = 11 Hz), 5.80 (1 H, s), 7.26–7.70 (20 H, m), 8.27 (1 H, brs); ^{13}C NMR (100.5 MHz, $CDCl_3$) δ 11.7, 19.5, 20.2, 27.2, 27.8, 49.8, 54.2, 60.9, 74.1, 90.3, 91.3, 110.1, 128.1, 128.3, 128.4, 130.4, 130.4, 130.6, 130.8, 132.5, 133.3, 134.4, 135.6, 135.9, 136.2, 149.8, 164.0; MS (FAB) m/z 795 (M + H^+); HRMS (FAB): Calcd for $C_{43}H_{51}N_2O_5S_2Si_2$ (M + H^+): 795.2778. Found: 795.2776.

1-[2-Thio-3,5-di-*O*-(*tert*-butyldiphenylsilyl)-2-*S*,4-*C*-{(*R*)-(benzoylsulfanyl)methylene}-β-D-ribofuranosyl]thymine (4). To a solution of compound **3** (200 mg, 0.25 mmol) in pyridine (2.5 mL) was added benzoyl chloride (0.088 mL, 0.76 mmol) and the resultant mixture was stirred at room temperature for 1 h under a N_2 atmosphere. After addition of H_2O, the reaction mixture was diluted with AcOEt, dried over Na_2SO_4, and concentrated. The crude product was purified by column chromatography ($CHCl_3/CH_3OH$ = 60/1) to give compound **4** (184 mg, 81%, over 2 steps) as a white foam; $[\alpha]_D^{23}$ +43.4 (*c* 1.0, CH_2Cl_2); IR ν_{max} (KBr): 1689, 2858, 2891, 2933, 3050, 3069 cm^{-1}; ^1H NMR (400 MHz, $CDCl_3$) δ 1.05– 1.14 (21 H, m), 3.07 (1 H, d, J = 2 Hz), 4.22 (2 H, s), 4.48 (1 H, s), 5.45 (1 H, s), 5.83 (1 H, s), 7.23–7.90 (26 H, m); ^{13}C NMR (100.5 MHz, $CDCl_3$) δ 11.4, 19.4, 20.0, 27.0, 27.4, 53.6, 54.0, 60.8, 74.0, 90.3, 91.7, 109.9, 127.5, 128.0, 128.0, 128.1, 128.1, 128.5, 128.9, 130.1, 130.2, 130.3, 130.4, 130.6, 132.1, 132.6, 133.1, 134.0, 134.3, 135.4, 135.8, 136.1, 149.6, 164.0, 191.2; MS (FAB) m/z 899 (M + H^+); HRMS (FAB): Calcd for $C_{50}H_{55}N_2O_6S_2Si_2$ (M + H^+): 899.3040. Found: 899.3073.

1-[2-Thio-2-*S*,4-*C*-{(*R*)-(benzoylsulfanyl)methylene}-β-D-ribofuranosyl]thymine (5). To a solution of compound **4** (64 mg, 0.071 mmol) in THF (0.71 mL) was added tetrabutylammonium fluoride (1.0 M in THF, 0.21 mL, 0.21 mmol) and acetic acid (0.061 mL, 1.1 mmol) and the resultant mixture was stirred at room temperature for 23 h. Furthermore, tetrabutylammonium fluoride (1.0 M in THF, 0.14 mL, 0.14 mmol) and acetic acid (0.041 mL, 0.7 mmol) was added to the mixture and the mixture was stirred at room temperature for 25 h. The reaction mixture was concentrated and the crude product was purified by column chromatography ($CHCl_3/CH_3OH$ = 20/1 to 10/1) and purified further by column chromatography (AcOEt/CH_3OH = 30/1) to give compound **5** (21 mg, 70%) as a white foam; $[\alpha]_D^{25}$ +192.9 (*c* 1.0, MeOH); IR ν_{max} (KBr): 1580, 1597, 1685, 2099, 2320, 2925, 3063, 3373 cm^{-1}; ^1H NMR (400 MHz, CD_3OD) δ 1.85 (3 H, s), 3.65 (1 H, s), 3.85 (1 H, d, J = 12 Hz), 3.91 (1 H, d, J = 12 Hz), 4.59 (1 H, d, J = 3 Hz), 5.33 (1 H, s), 5.88 (1 H, s), 7.47– 7.51 (2 H, m), 7.61– 7.65 (1 H, m), 7.92– 7.94 (2 H, m), 8.12 (1 H, s); ^{13}C NMR (100.5 MHz, CD_3OD) δ 12.7, 54.7, 58.5, 72.6, 91.4, 92.8, 110.1, 128.3, 130.0, 135.1, 137.3, 137.6, 152.0, 166.5, 192.3; MS (FAB) m/z 423 (M + H^+); HRMS (FAB): Calcd for $C_{18}H_{19}N_2O_6S_2$ (M + H^+): 423.0685. Found: 423.0681.

1-[2-Thio-5-*O*-(4,4′-dimethoxytrityl)-2-*S*,4-*C*-{(*R*)-(benzoylsulfanyl)methylene}-β-D-ribofuranosyl]thymine (6). To a solution of compound **5** (260 mg, 0.61 mmol) in pyridine (3.1 mL) was added 4,4′-dimethoxytrityl chloride (310 mg, 0.92 mmol) and the resultant mixture was stirred at room temperature for 2.5 h under a N_2 atmosphere. Furthermore 4,4′-dimethoxytrityl chloride (210 mg, 0.61 mmol) was added to the mixture and the mixture was stirred at room temperature for 30 min. After addition of H_2O, the reaction mixture was diluted with CH_2Cl_2, dried over Na_2SO_4, and concentrated. The crude product was purified by column chromatography (0.5% triethylamine in n-hexane/AcOEt = 1/1 to AcOEt only) to give compound **6** (350 mg, 79%) as a white foam; $[\alpha]_D^{24}$ –100.4 (*c* 1.0, CH_2Cl_2); IR ν_{max} (KBr): 1508, 1580, 1608, 1685, 1973, 2044, 2321, 2835, 2933, 3066, 3412 cm^{-1}; ^1H NMR (400 MHz, $CDCl_3$) δ 1.01–1.14 (21 H, m), 3.08 (1 H, d, J = 2 Hz), 4.22 (2 H, s), 4.48 (1 H, d, J = 2 Hz), 5.45 (1 H, s), 5.83 (1 H, s), 7.26–7.96 (26 H, m); ^{13}C NMR (100.5 MHz, $CDCl_3$) δ 12.3, 54.0, 54.0, 55.4, 59.8, 73.3, 87.5, 90.0, 91.1, 110.5, 113.5, 127.3, 127.5, 128.2, 128.3, 128.9, 130.2, 134.2, 134.8, 135.0, 135.1, 136.1, 144.1, 150.2, 158.8, 158.8, 164.1, 191.0; MS (FAB) m/z 747 (M + Na^+); HRMS (FAB): Calcd for $C_{39}H_{36}N_2NaO_8S_2$ (M + Na^+): 747.1811. Found: 747.1821.

1-[2-Thio-3-*O*-{2-cyanoethoxy(diisopropylamino)phosphino}-5-*O*-(4,4′-dimethoxytriryl)-2-*S*,4-*C*-{(*R*)-(benzoylsulfanyl)methylene}-β-D-ribofuranosyl]thymine (7). To a solution of compound **6** (350 mg, 0.48 mmol) in acetonitrile (8.8 mL) was added *N*,*N*-diisopropylethylamine (0.34 mL, 1.9 mmol) and *N*,*N*-diisopropylamino-2-cyanoethylphosphino chloridite (0.22 mL, 0.97 mmol) and the resultant mixture was stirred at 0 °C for 2 h under a N_2 atmosphere. The reaction mixture was concentrated and the crude product was purified by column chromatography (0.5% triethylamine in n-hexane/AcOEt = 1/1 to 1/2) to give compound **7** (290 mg, 66%) as a white foam; ^{31}P NMR (161.8 MHz, $CDCl_3$) δ 150.0, 150.4; MS (FAB) m/z 925 (M + H^+); HRMS (FAB): Calcd for $C_{48}H_{54}N_4O_9PS_2$ (M + H^+): 925.3070. Found: 925.3076.

ON synthesis

Synthesis of the thiol-containing BNA-modified ONs was performed on an Applied Biosystems Expedite™ 8909 Nucleic Acid Synthesis System on a 1.0 μmol scale using a phosphoramidite coupling protocol and 5-[3,5-bis(trifluoromethyl)phenyl]-1*H*-tetrazole as the activator. The concentration of phosporamidite **7** was 0.10 M and its coupling time was 20 min, while the concentration of each unmodified phosporamidite was 0.067 M and their coupling times were 90 s. The solid-supported ONs (DMTr-off) were treated with 50 mM K_2CO_3 and 100 mM 2,2′-dithiodipyridine in CH_3OH at room temperature for 2.5 h, then neutralized by 5% acetic acid and concentrated. The crude ONs were roughly purified with a GE Healthcare Nap 10 column, and then carefully by RP-HPLC on a Waters XBridge™ OST C18 2.5 μm (10 × 50 mm) using MeCN in 0.1 M triethylammonium acetate buffer (pH = 7.0). The purity of the ONs was analyzed by RP-HPLC on a Waters XBridge™ Shield RP 18 2.5 μm (4.6 × 50 mm) and characterized by MALDI-TOF mass spectrometry. The overall yields were 8.4% for ON **8** and 16.6% for ON **9** calculated from the UV absorbance at 260 nm.

General procedure for solution-phase conjugation of ONs

Thioether-linked conjugation. 500 μM ON **8** or **9** (12 μL, 6 nmol) was treated with 10 mM dithiothreitol (DTT) dissolved in 100 mM sodium phosphate buffer (pH = 8.0) (60 μL, 0.6 μmol) at room temperature for 2 h to give ON **10** or **11**, then, 5% acetic acid (3.4 μL) was added, and 1 M primary halogenoalkyl derivative in DMF (1.8 μL, 1.8 μmol) was added to the solution to afford a thioether-linked conjugate. The reaction was analyzed by RP-HPLC. After completing the reaction, the ON was precipitated by adding 5 volumes of ethanol. The mixture was kept at 0 °C for 30 min, centrifuged at 13 200 rpm for 15 min at 4 °C, and the resulting supernatant solution was removed. The obtained ON conjugates were purified by RP-HPLC and characterized by MALDI-TOF mass spectrometry. Each conjugation yield was calculated from UV absorption at 260 nm of the ON conjugate.

Disulfide-linked conjugation. A solution of 500 μM ON **8** or **9** (10 μL, 5 nmol) in 0.1 mM TEAA buffer (pH = 7.0, 22 μL) was treated with 10 mM thiol compound in DMF (1.25 μL, 1.25 μmol) at room temperature for 24 h to give a disulfide-linked conjugate. The method of reaction analysis, purification, characterization, and yield calculation was the same as thioether-linked conjugates.

Thermal denaturation experiments. Thermal denaturation experiments were carried out on SHIMADZU UV-1650 and UV-1800 spectrometers equipped with a T_m analysis accessory. For the duplex formation study, equimolecular amounts of the target ssDNA/ssRNA and ONs were dissolved in 10 mM sodium phosphate buffer (pH = 7.2) containing 100 mM NaCl to give a final strand concentration of 4.0 μM. The ON/target samples were then annealed by heating at 90 °C followed by slow cooling to room temperature. The melting profile was recorded at 260 nm from 5 to 90 °C at a scan rate of 0.5 °C/min. T_m values for ON **10** were measured on the condition that ON **8** and target ssDNA/ssRNA were dissolved in 11 mM sodium phosphate buffer (pH = 7.4) containing 111 mM NaCl, annealed by heating at 90 °C followed by slow cooling to room temperature, and then 4 mM tris(2-carboxyethyl)phosphine hydrochloride (TCEP-HCl) aqueous solution was added to the mixtures to give a final strand concentration of 4.0 μM, pH 7.2.[35]

Nuclease resistance study. CAVP (Amersham Pharmacia Biotech, NJ, United States) (0.35 μg) was added to a solution of ON (750 pmol) in 50 mM Tris-HCl buffer (pH = 8.5) containing 10 mM $MgCl_2$. ON **11** was prepared by treating ON **9** with DTT (100 eq.) and used without any purification. The cleavage reaction was carried out at 37 °C. At several time points, a portion of each reaction mixture was removed and heated to 90 °C for 2 min to inactivate the nuclease. The amount of intact ON was then plotted against the exposure time to obtain the ON degradation curve with time. The fitted line for each ON degradation was obtained.

Acknowledgements

This work was supported by a Grant-in-Aid for Challenging Exploratory Research (22651076) from the Japan Society for the Promotion of Science (JSPS), a Grant-in-Aid for Scientific Research on Innovative Area (22136006) from the Ministry of Education, Culture, Sports, Science and Technology, Japan (MEXT), and the Program for Promotion of Fundamental Studies in Health Sciences of the National Institute of Biomedical Innovation (NIBIO).

Notes and references

1 S. Brantl, *Biochim. Biophys. Acta, Gene Struct. Expression*, 2002, **1575**, 15.
2 X. Chen, N. Dudgeon, L. Shen and J. H. Wang, *Drug Discovery Today*, 2005, **10**, 587; R. Juliano, J. Bauman, H. Kang and X. Ming, *Mol. Pharmaceutics*, 2009, **6**, 686; C. V. Pecot, G. A. Calin, R. L. Coleman, G. L. Berestein and A. K. Sood, *Nat. Rev. Cancer*, 2011, **11**, 59; T. Yamamoto, M. Nakatani, K. Narukawa and S. Obika, *Future Med. Chem.*, 2011, **3**, 339.
3 S. M. A. Rahman, T. Imanishi and S. Obika, *Chem. Lett.*, 2009, **38**, 512; S. Obika, S. M. A. Rahman, A. Fujisaka, Y. Kawada, T. Baba and T. Imanishi, *Heterocycles*, 2010, **81**, 1347.
4 M. Petersen and J. Wengel, *Trends Biotechnol.*, 2003, **21**, 74; J. Wengel, M. Petersen, M. Frieden and T. Koch, *Lett. Pept. Sci.*, 2003, **10**, 237; H. Kaur, B. R. Babu and S. Maiti, *Chem. Rev.*, 2007, **107**, 4672; R. N. Veedu and J. Wengel, *Chem. Biodiversity*, 2010, **7**, 536.
5 M. Manoharan, *Antisense Nucleic Acid Drug Dev.*, 2002, **12**, 103; R. Juliano, M. R. Alam, V. Dixit and H. Kang, *Nucleic Acids Res.*, 2008, **36**, 4158.
6 S. Obika, D. Nanbu, Y. Hari, J. Andoh, K. Morio, T. Doi and T. Imanishi, *Tetrahedron Lett.*, 1998, **39**, 5401.
7 S. K. Singh, P. Nielsen, A. A. Koshkin and J. Wengel, *Chem. Commun.*, 1998, 455.
8 F. E. Alemdaroglu and A. Herrmann, *Org. Biomol. Chem.*, 2007, **5**, 1311; S. H. Weisbrod and A. Marx, *Chem. Commun.*, 2008, 5675; Y. Singh, P. Murat and E. Defrancq, *Chem. Soc. Rev.*, 2010, **39**, 2054; C. M. Niemeyer, *Angew. Chem., Int. Ed.*, 2010, **49**, 1200.
9 L. Lacerda, A. Bianco, M. Prato and K. Kostarelos, *J. Mater. Chem.*, 2008, **18**, 17; Y. Song, X. Xu, K. W. MacRenaris, X.-Q. Zhang, C. A. Mirkin and T. J. Meade, *Angew. Chem., Int. Ed.*, 2009, **48**, 9143; T. Ihara, A. Uemura, A. Futamura, M. Shimizu, N. Baba, S. Nishizawa, N. Teramae and A. Jyo, *J. Am. Chem. Soc.*, 2009, **131**, 1386; D. Ge and R. Levicky, *Chem. Commun.*, 2010, **46**, 7190.
10 H. Lönnberg, *Bioconjugate Chem.*, 2009, **20**, 1065; K. Lu, Q.-P. Duan, L. Ma and D.-X. Zhao, *Bioconjugate Chem.*, 2010, **21**, 187; A. V. Ustinov, I. A. Stepanova, V. V. Dubnyakova, T. S. Zatsepin, E. V. Nozhevnikova and V. A. Korshun, *Russ. J. Bioorg. Chem.*, 2010, **36**, 401.
11 S. K. Hamilton, A. L. Sims, J. Donavan and E. Harth, *Polym. Chem.*, 2011, **2**, 441; J. H. Jeong, H. Mok, Y. K. Oh and T. G. Park, *Bioconjugate Chem.*, 2009, **20**, 5; F. Meng, W. E. Hennink and Z. Zhong, *Biomaterials*, 2009, **30**, 2180.
12 A. Muratovska and M. R. Eccles, *FEBS Lett.*, 2004, **558**, 63; R. L. Juliano, *Ann. N. Y. Acad. Sci.*, 2006, **1082**, 18; F. Meng, W. E. Hennink and Z. Zhong, *Biomaterials*, 2009, **30**, 2180.
13 A. Ono, A. Dan and A. Matsuda, *Bioconjugate Chem.*, 1993, **4**, 499; J. Hovinen, A. Guzaev, E. Azhayeva, A. Azhayav and H. Lönnberg, *J. Org. Chem.*, 1995, **60**, 2205; P. Grünefeld and C. Richert, *J. Org. Chem.*, 2004, **69**, 7543.
14 M. Manoharan, C. J. Guinosso and P. D. Cook, *Tetrahedron Lett.*, 1991, **32**, 7171; M. Manoharan, K. L. Tivel and W. Pfleiderer, *Tetrahedron Lett.*, 1995, **36**, 3651; J.-T. Hwang and M. M. Greenberg, *Org. Lett.*, 1999, **1**, 2021; M. Beban and P. S. Miller, *Bioconjugate Chem.*, 2000, **11**, 599; J.-T. Hwang and M. M. Greenberg, *J. Org. Chem.*, 2001, **66**, 363; N. Kalra, B. R. Babu, V. S. Parmar and J. Wengel, *Org. Biomol. Chem.*, 2004, **2**, 2885.
15 M. D. Sørensen, M. Petersen and J. Wengel, *Chem. Commun.*, 2003, 2130.
16 A. W. I. Stephenson, N. Bomholt, A. C. Partridge and V. V. Filichev, *ChemBioChem*, 2010, **11**, 1833; T. Ehrenschwender, B. R. Varga, P. Kele and H.-A. Wagenknecht, *Chem.-Asian J.*, 2010, **5**, 1761.
17 C. Dohno and I. Saito, *ChemBioChem*, 2005, **6**, 1075; A. Kiviniemi, P. Virta and H. Lönnberg, *Bioconjugate Chem.*, 2008, **19**, 1726.
18 M. J. Davies, A. Shah and I. J. Bruce, *Chem. Soc. Rev.*, 2000, **29**, 97; S. Dey and T. L. Sheppard, *Org. Lett.*, 2001, **3**, 3983.

19 J. Fidanza and L. W. McLaughlin, *J. Org. Chem.*, 1992, **57**, 2340; M. Chen and K. V. Gothelf, *Org. Biomol. Chem.*, 2008, **6**, 908.
20 K. Yamana, R. Iwase, S. Furutani, H. Tsuchida, H. Zako, T. Yamaoka and A. Murakami, *Nucleic Acids Res.*, 1999, **27**, 2387; T. Bryld, T. Højland and J. Wengel, *Chem. Commun.*, 2004, 1064; T. S. Kumar, A. S. Madsen, M. E. Østergaard, S. P. Sau, J. Wengel and P. J. Hrdlicka, *J. Org. Chem.*, 2009, **74**, 1070; M. E. Østergaard, D. C. Guenther, P. Kumar, B. Baral, L. Deobald, A. J. Paszczynski, P. K. Sharma and P. J. Hrdlicka, *Chem. Commun.*, 2010, **46**, 4929.
21 A. S. Jørgensen, K. I. Shaikh, G. Enderlin, E. Ivarsen, S. Kumar and P. Nielsen, *Org. Biomol. Chem.*, 2011, **9**, 1381.
22 T. Baba, T. Kodama, K. Mori, T. Imanishi and S. Obika, *Chem. Commun.*, 2010, **46**, 8058.
23 L. B. Barron, K. C. Waterman, P. Filpiak, G. L. Hug, T. Nauser and C. Schöeich, *J. Phys. Chem. A*, 2004, **108**, 2247; L. B. Barron, K. C. Waterman, T. J. Offerdahl, E. Munson and C. Schöeich, *J. Phys. Chem. A*, 2005, **109**, 9241.
24 R. Kumar, S. K. Singh, A. A. Koshkin, V. K. Rajwanshi, M. Meldgaard and J. Wengel, *Bioorg. Med. Chem. Lett.*, 1998, **8**, 2219; S. K. Singh, R. Kumar and J. Wengel, *J. Org. Chem.*, 1998, **63**, 6078; D. S. Pedersen and T. Koch, *Synthesis-Stuttgart*, 2004, 578; K. Fluiter, M. Frieden, J. Vreijling, C. Rosenbohm, M. B. De Wissel, S. M. Christensen, T. Koch, H. Ørum and F. Baas, *ChemBioChem*, 2005, **6**, 1104.
25 M. Nishida, T. Baba, T. Kodama, A. Yahara, T. Imanishi and S. Obika, *Chem. Commun.*, 2010, **46**, 5283.
26 W. H. A. Kuijpers and C. A. A. van Boeckel, *Tetrahedron*, 1993, **49**, 10931.
27 Q. Zhang and J. W. Kelly, *Biochemistry*, 2003, **42**, 8756.
28 A. Bajaj, P. Kondaiah and S. Bhattacharya, *J. Med. Chem.*, 2008, **51**, 2533.
29 M. W. Johannsen, L. Crispino, M. C. Wamberg, N. Kalra and J. Wengel, *Org. Biomol. Chem.*, 2011, **9**, 243.
30 B. Mestre, M. Pitie, C. Loup, C. Claparols, G. Pratviel and B. Meunier, *Nucleic Acids Res.*, 1997, **25**, 1022.
31 V. A. Korshun, D. A. Stetsenko and M. J. Gait, *J. Chem. Soc., Perkin Trans. 1*, 2002, 1092.
32 W. E. Razzell, *Methods Enzymol.*, 1963, **6**, 236.
33 Y. Liu, J. Xu, M. Karimiahmadabadi, C. Zhou and J. Chattopadhyaya, *J. Org. Chem.*, 2010, **75**, 7112.
34 S. Park, M. Seetharaman, A. Ogdie, D. Ferguson and N. Tretyakova, *Nucleic Acids Res.*, 2003, **31**, 1984.
35 A reducing agent TCEP-HCl was added in order to reduce ON **8** and generate ON **10**. Acidic TCEP-HCl aqueous solution was added into the annealed mixtures, therefore the final pH and the concentrations of sodium phosphate buffer and NaCl conditions for the UV melting experiment were equal to the other experiments.

2．糖部架橋型核酸の医薬への応用

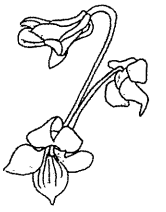

小比賀　聡*

核酸医薬の開発においては，優れた人工核酸の創製が必要不可欠である。核酸分子は，相補的な配列を持つ鎖と配列特異的に結合するという特性を元来有しているが，この特性を損なわず，あるいはむしろ高めつつ，生体内においても十分安定に存在できる人工核酸の開発が世界中で活発に展開されている。我々が開発してきた糖部架橋型核酸もその一つであり，糖部のコンホメーションをN型と呼ばれるRNA類似の構造に厳密に固定している。その結果，相補鎖RNAに対する高い結合親和性や生体内での優れた安定性を獲得するに至った。

この糖部架橋型人工核酸の一種である2',4'-BNA/LNA(2',4'-Bridged Nucleic Acid/Locked Nucleic Acid)は，RNAを標的とした核酸医薬として欧米を中心に臨床試験が展開されている。

1．はじめに

これまで低分子化合物が医薬品の中心的役割を担ってきたが，最近になってこれら低分子化合物を基盤とした新薬の開発にやや陰りが見られるようになってきた。

生命現象の解明が進むにつれ，タンパク質や核酸といった生体高分子同士の相互作用が疾病の発現に関わっていることが徐々に明らかとなってきた。しかし，低分子化合物を用いて，こうした生体高分子同士の相互作用を制御することは必ずしも容易ではないという点が，その一因として考えられる。

一方，核酸医薬の多くは，標的とするタンパク質の発現そのものを遺伝子レベルで抑制する。そのため，従来の低分子医薬では困難であった生体高分子間の相互作用の抑制という課題をも実現することが可能である。

本稿では，我々が開発してきた糖部架橋型人工核酸の創薬への応用例，特にRNAを標的とした核酸医薬開発の現状について概説したい。

2．RNAを標的とした核酸医薬に求められる特性

DNAに刻まれた遺伝情報は，**mRNA**(messenger RNA)へ転写され，さらにタンパク質へと翻訳される。一方，最近になってタンパク質へとコードされないRNA，いわゆるノンコーディングRNA(**ncRNA**)が，遺伝子の発現制御に大きく関わっていることも分かってきた[1)2)]。RNAを標的とした核酸医薬は，細胞の中でmRNAやncRNAと配列特異的に結合し，病気の原因となるタンパク質の発現を抑制することで機能する。(**図1**)。そのため，標的となるRNAと配列特異的にかつ強固に結合することが，核酸医薬には必要不可欠である。また生体内には核酸を分解する酵素が多

*大阪大学大学院薬学研究科生物有機化学分野・教授（おびか・さとし）

く存在し，天然のDNAやRNAは速やかに分解を受けるため，核酸医薬の素材として利用することは困難である。そのため，核酸医薬には生体内における高い安定性が求められる。現在，臨床試験が進められている核酸医薬の多くは[3]，生体内の安定性を高めるためリン酸ジエステル結合をホスホロチオアート化するという工夫がなされている。一方，標的となる臓器への移行性（体内動態）の制御も核酸医薬の重要な課題と考えられている。

上記のホスホロチオアート化を含め，さまざまな化学修飾により核酸医薬の体内動態を制御することは徐々に可能となりつつあるが[4]，これら核酸医薬自身の化学修飾に加えて，核酸医薬を望みの臓器に送達するためのデリバリー技術の確立が求められている。

3．架橋型人工核酸とは

1997年，我々大阪大学のグループでは核酸の2'位酸素原子と4'位炭素原子を架橋した新たな人工核酸，**2',4'-BNA**（2',4'-Bridged Nucleic Acid）[5]，別名**LNA**（Locked Nucleic Acid）[6]，の開発に世界に先駆け成功した。（**図2**）。その合成については，原著論文[5][7]のほか，既にいくつかの総説としてまとめているので，そちらを参照していただきたい[8]～[10]。

架橋型人工核酸の導入によって核酸の物性は大きく変化し，医薬素材としても非常に有望であることが分かってきた。例えば，標的RNAとの結合親和性に関する我々の実験から，12merのDNAに2',4'-BNA/LNAを6カ所導入した場合，約10万倍も向上することが明らかとなった[11]。さらに，核酸を分解する酵素に対する耐性も大きく改善した[12]。このうち前者については，当初の我々の分子設計通り，2',4'-BNA/LNAの糖部コンホメーションが厳密にRNAと同じN型に固定化されていることによる。一方，後者については，架橋部分の立体的な効果から核酸分解酵素がリン酸ジエステル結合に接近することを阻害しているためであると考えられる。

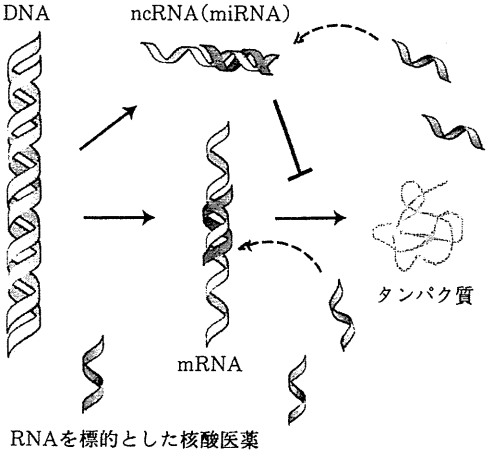

図1　RNAを標的とした核酸医薬の作用様式
細胞内において，RNAを標的とした核酸医薬は，メッセンジャーRNA（mRNA）やノンコーディングRNA（ncRNA）等の一本鎖RNAと配列特異的に結合し，それらRNAの機能を抑制することで遺伝子発現を制御する．
（筆者作成）

4．架橋型人工核酸を用いた核酸医薬開発の現状

架橋型人工核酸の開発は，我々の最初の報告の後に世界中で活発に行なわれてきた[9][10]。その中で，初代の架橋型人工核酸（2',4'-BNA/LNA）は既にデンマークのSantaris Pharma社を中心に臨床試験が進められている。（**図3**）[13]。そのうち代表的な2例を以下に紹介したい。

1）SPC3649（miravirsen）[14][15]

SPC3649はC型肝炎治療薬としてSantaris Pharma社により開発が進められている核酸医薬である。**HCV**（C型肝炎ウイルス）の増殖に深く関わっているmicroRNA（ncRNAの一種）であるmiR-122を標的としたもので，当初は，血中のコレステロール**LDL-C**（low density lipoprotein cholesterol）を低減する作用があるとして注目を集めていた[14]。これに加えて，最近の報告では，HCVに慢性感染したチンパンジーへの投与により，肝臓および血中でのHCV量を大幅に低減す

2',4'-BNA：2',4'-Bridged Nucleic Acid，**LNA**：Locked Nucleic Acid，**HCV**：C型肝炎ウイルス
LDL-C：low density lipoprotein cholesterol

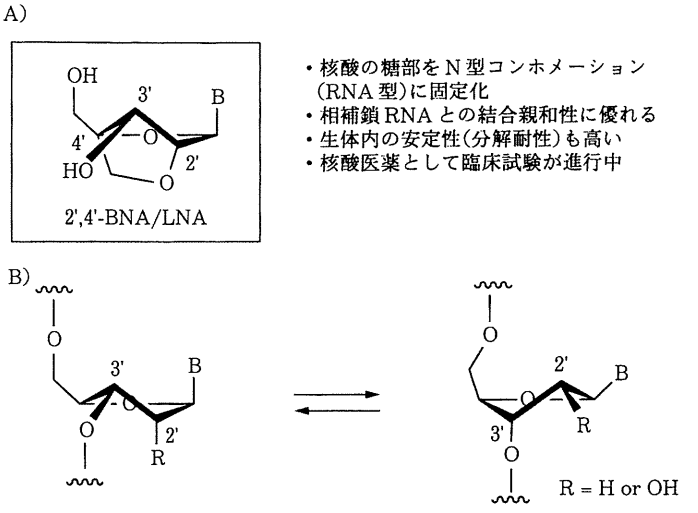

図2　A）架橋型人工核酸 2',4'-BNA/LNA の化学構造とその特徴
B）核酸（RNA，DNA）の糖部コンホメーション

核酸の糖部2'位と4'位の間に化学的な架橋を施すことで，通常はRNA型（N型）とDNA型（S型）の両方をとることができる糖部の構造を厳密にRNA型（N型）に固定化することができる．その結果，RNAを標的とした核酸医薬に相応しい優れた特性が得られる．

2',4'-BNA/LNA：2',4'-Bridged Nucleic Acid/Locked Nucleic Acid

（筆者作成）

ることが見出されている。またこの前臨床試験では，顕著な副作用は認められておらず，さらには最高で数カ月もの間効果が持続する等，極めて良好な結果が示されている[15]。現行のHCV治療薬としては，インターフェロンαやリバビリンが知られているが，これらは著効率が十分ではないという問題を残していたため，新たなメカニズムで作用する核酸医薬SPC3649には大きな期待が寄せられている。なお，このSPC3649については現在フェーズ2の臨床試験が進められている。（**図3**）[13]。

2）SPC4955[16]

一方，SPC4955は同じくSantaris Pharma社により，脂質異常症（高コレステロール血症）治療薬として開発されている核酸医薬である。これは，LDL-Cの主要構成成分である**ApoB**（apolipoprotein B）のmRNAを標的としたアンチセンス核酸であり，肝臓でのApoB合成を阻害することで血中LDL-Cの低減をもたらす。従来のアンチセンス核酸には，18～22mer程度の鎖長のオリゴヌクレオチドが主に用いられてきたが，2',4'-BNA/LNAアンチセンスにおいては，その優れたRNA結合親和性により，12～14mer程度の鎖長のオリゴヌクレオチドでも十分な効果を発揮することが示された。特に，*in vivo*での薬効は鎖長の長いアンチセンス核酸を凌ぐものであった。これは，従来のアンチセンス核酸の配列設計を根本的に見直すきっかけとなる重要な知見であるとともに，アンチセンス医薬のコスト低減につながるものと期待される。このSPC4955については現在フェーズ1段階にあり，今後の進展が期待される。（**図3**）[13]。

ApoB：apolipoprotein B

COMPOUND	TARGET	INDICATION	LEAD DISCOVERY	PRE-CLINICAL	PHASE I	PHASE II	PHASE III
miravirsen (SPC3649)	miR-122	Hepatitis C	○○○○○○○	○○○○○○○	○○○○○○○	○○○	
EZN-2968[1]	HIF-1a	Solid Tumors	○○○○○○○	○○○○○○○	○○○○○○○		
EZN-3042[1]	Survivin	Cancer	○○○○○○○	○○○○○○○	○○○○○		
EZN-4176[1]	Androgen Receptor	Cancer	○○○○○○○	○○○○○○○	○○○		
SPC4955	Apolipoprotein B	Hypercholesterolemia	○○○○○○○	○○○○○○○	○○○		
PCSK9 Program	PCSK9	Hypercholesterolemia	○○○○○○○	○○○○○○○			
Enzon Programs[1]	Beta-catenin, Her-3	Cancer	○○○○○				
Pfizer Programs[2]	Undisclosed	Various	○○○○○				
Shire Programs[2]	Undisclosed	Rare Genetic Disorders	○○○○○				
miRagen Programs[2]	Undisclosed	Cardiovascular Disease	○○○○○				
GSK Programs[2]	Undisclosed	Viral Diseases	○○○○○				

Santaris Compounds □ Partnerd Compounds □

[1]Santaris Pharma A/S retains commercial rights in Europe, US and rest of world partnered with Enzon
[2]Worldwide commercial rights partnered

図3 Santaris Pharma 社（デンマーク）における架橋型人工核酸の医薬品開発状況

Santaris Pharma 社では，架橋型人工核酸（2',4'-BNA/LNA）を用いた核酸医薬の開発を進めている．miravirsen（SPC3649）およびSPC4955以外にも，がんをはじめとした，いくつかの核酸医薬が臨床試験に進んでいる．

（文献13より転載）

Vol. 48, No. 1, 2012/p.68

5．おわりに

架橋型人工核酸を搭載したオリゴヌクレオチドは標的RNAとの結合親和性が大きく向上することから，特にRNAを標的とした核酸医薬素材として有望である。核酸医薬の問題点の一つにそのコストがあげられるが，2',4'-BNA/LNAの合成に関しては十分な最適化が進められてきた。さらに，上述のように，従来よりも短い鎖長で十分な薬効を示すことが明らかとなっており，コストの問題に関してはある程度の目処がついたと言ってもいいであろう。一方，核酸医薬が抱えるその他の問題として，標的臓器へのデリバリー技術が十分ではないという点があげられる。架橋型人工核酸をはじめとする各種の人工核酸の開発とともに，デリバリー技術が一段と成熟化することで，今後ますます核酸医薬の利用範囲は広まっていくであろう。

文　献

1) 河合剛太，金井昭夫 編："機能性Non-coding RNA". クバプロ，東京. 2006.
2) Sayed D, Abdellatif M : MicroRNAs in development and disease. Physiol Rev **91** : 827-887, 2011.
3) Yamamoto T, et al : Antisense drug discovery and development. Future Med Chem **3** : 339-365, 2011.
4) Kuboyama T, et al : Stoichiometry-focused ^{18}F-labeling of alkyne-substituted oligonucleotides using azido ([^{18}F]fluoromethyl) benzenes by Cu-catalized Huisgen reaction. Bioorg Med Chem **19** : 249-255, 2011.
5) Obika S, et al : Synthesis of 2'-*O*,4'-*C*-methyleneuridine and -cytidine. Novel bicyclic nucleosides having a fixed C3'-*endo* sugar puckering. Tetrahedron Lett **38**:8735-8738, 1997.
6) Singh SK, et al : LNA (locked nucleic acids) : synthesis and high-affinity nucleic acid recognition. Chem Commun : 455-456, 1998.
7) Obika S, et al : 2'-*O*,4'-*C*-Methylene bridged nucleic acid (2',4'-BNA) : synthesis and triplex-forming properties. Bioorg Med Chem **9** : 1001-1011, 2001.
8) 小比賀 聡，今西 武：糖部架橋型核酸医薬の合成とその性質．"核酸医薬の最前線" 和田 猛 監修．シーエムシー出版，東京．p.55-66, 2009.
9) Rahman SMA, Imanishi T, Obika S : Synthesis of several types of bridged nucleic acids. Chem Lett **38** : 512-517, 2009.
10) Obika S, et al : Bridged nucleic acids : development, synthesis and properties. Heterocycles **81** : 1347-1392, 2010.
11) Obika S, et al : Stability and structural features of the duplexes containing nucleoside analogues with a fixed N-type conformation, 2'-*O*,4'-*C*-methyleneribonucleosides. Tetrahedron Lett **39** : 5401-5404, 1998.
12) Imanishi T, Obika S : Syntheses and properties of novel conformationally restrained nucleoside analogues. J Syn Org Chem Jpn **57** : 969-980, 1999.
13) Santaris Pharma 社ホームページ. http://www.santaris.com/product-pipeline
14) Elmén, et al : LNA-mediated microRNA silencing in non-human primates. Nature **452** : 896-899, 2008.
15) Lanford RE, et al : Therapeutic silencing of microRNA-122 in primates with chronic hepatitis C virus infection. Science **327** : 198-201, 2010.
16) Straarup EM, et al : Short locked nucleic acid antisense oligonucleotides potently reduce apolipoprotein B mRNA and serum cholesterol in non-human primates. Nucleic Acids Res **38** : 7100-7111, 2010.

Citation: Molecular Therapy–Nucleic Acids (2012) 1, e1; doi:10.1038/mtna.2012.16

www.nature.com/mtna

Cholesterol-lowering Action of BNA-based Antisense Oligonucleotides Targeting PCSK9 in Atherogenic Diet-induced Hypercholesterolemic Mice

Tsuyoshi Yamamoto[1,2], Mariko Harada-Shiba[2], Moeka Nakatani[1,2], Shunsuke Wada[2,3], Hidenori Yasuhara[1,2], Keisuke Narukawa[1], Kiyomi Sasaki[3], Masa-Aki Shibata[4], Hidetaka Torigoe[3], Tetsuji Yamaoka[5], Takeshi Imanishi[6] and Satoshi Obika[1]

[Q1] **Recent findings in molecular biology implicate the involvement of proprotein convertase subtilisin/kexin type 9 (PCSK9) in low-density lipoprotein receptor (LDLR) protein regulation. The cholesterol-lowering potential of anti-PCSK9 antisense oligonucleotides (AONs) modified with bridged nucleic acids (BNA-AONs) including 2′,4′-BNA (also called as locked nucleic acid (LNA)) and 2′,4′-BNA^{NC} chemistries were demonstrated both *in vitro* and *in vivo*. An *in vitro* transfection study revealed that all of the BNA-AONs induce dose-dependent reductions in PCSK9 messenger RNA (mRNA) levels concomitantly with increases in LDLR protein levels. BNA-AONs were administered to atherogenic diet-fed C57BL/6J mice twice weekly for 6 weeks; 2′,4′-BNA-AON that targeted murine PCSK9 induced a dose-dependent reduction in hepatic PCSK9 mRNA and LDL cholesterol (LDL-C); the 43% reduction of serum LDL-C was achieved at a dose of 20 mg/kg/injection with only moderate increases in toxicological indicators. In addition, the serum high-density lipoprotein cholesterol (HDL-C) levels increased. These results support antisense inhibition of PCSK9 as a potential therapeutic approach. When compared with 2′,4′-BNA-AON, 2′,4′-BNA^{NC}-AON showed an earlier LDL-C–lowering effect and was more tolerable in mice. Our results validate the optimization of 2′,4′-BNA^{NC}-based anti-PCSK9 antisense molecules to produce a promising therapeutic agent for the treatment of hypercholesterolemia.**

Molecular Therapy–Nucleic Acids (2012) **1**, e1; doi:10.1038/mtna.2012.16; published online 00 Month 2012

Introduction

Statins are lipid-lowering drugs that achieve a strong reduction of serum low-density lipoprotein cholesterol (LDL-C) mainly *via* the indirect activation of LDL receptor (LDLR)-mediated hepatic uptake of LDL from the blood.[1,2] The development of drugs that directly regulate the expression of hepatic LDLR would thus be a compelling strategy to obtain the efficacy of statin-induced LDL-C reduction while compensating for potential weaknesses of statin therapy, such as severe adverse effects (e.g., myopathy). The molecular basis of LDLR regulation as well as cholesterol maintenance has been enthusiastically elucidated,[2–7] and several causative molecules of hypercholesterolemia relevant to the direct regulation of LDLR function have recently been identified.[8–11] Proprotein convertase subtilisin/kexin type 9 (PCSK9), which was recently identified as the third gene relevant to autosomal dominant hypercholesterolemia,[10] is involved in the maintenance of cholesterol balance. A number of human mutations in PCSK9 have been reported. Gain-of-function mutations are associated with autosomal dominant hypercholesterolemia, whereas loss-of-function mutations are relevant to low blood levels of LDL-C.[12] Recent findings have suggested the involvement of PCSK9 in LDLR regulation. PCSK9 is synthesized mainly in the liver, small intestine, and kidney as a 72-kDa soluble zymogen that subsequently undergoes autocatalytic cleavage into an active form. The active 63-kDa enzyme in complex with the cleaved prodomain is secreted into the bloodstream. Secreted PCSK9 directly binds to an extracellular part of the LDLR. The LDLR–PCSK9 complex is transported from the cell surface to the endosomal system for digestion. PCSK9 forms a stable complex with LDLR in lysosomes, which disturbs the recycling of LDLR to reduce LDL uptake.[4,13,14] PCSK9 would be a pivotal regulator of LDLR and an attractive target for lipid-lowering therapy, although some molecular functions of PCSK9 remain unknown.

To achieve PCSK9 inhibition, several "molecular-targeted" approaches have been attempted. To our knowledge, berberine, an isoquinoline plant alkaloid, is the sole small molecule that achieves suppression of PCSK9 expression at the transcriptional level.[15–17] An antibody against secreted PCSK9 efficiently reduced the serum LDL-C levels of mice and monkeys.[18] [Q3] Small interfering RNA formulated in a lipidoid nanoparticle can induce liver-specific reduction of PCSK9 messenger RNA (mRNA) and serum total cholesterol levels in wild-type mice.[19] These proof-of-concept studies demonstrate the therapeutic promise of PCSK9-targeted therapies. Antisense inhibition of PCSK9 is superior to the aforementioned strategies because antisense oligonucleotide (AON) molecules can deactivate intrahepatic mRNA as well as proteins in the blood; in addition, they target the liver *via* a simple delivery methodology. Graham *et al.* showed that 2′-*O*-methoxyethyl-modified phosphorothioate oligonucleotide (MOE) (100 mg/kg/week) administered for a 6-week period to mice fed a high-fat diet reduced

[Q2] [1]Graduate School of Pharmaceutical Sciences, Osaka University, Suita, Japan; [2]Department of Molecular Innovation in Lipidology, National Cerebral and Cardiovascular Center Research Institute, Suita, Japan; [3]Faculty of Science, Tokyo University of Science, Shinjuku-ku, Japan; [4]Faculty of Health Science, Osaka Health Science University, Osaka, Japan; [5]Department of Biomedical Engineering, National Cerebral and Cardiovascular Center Research Institute, Suita, Japan; [6]BNA Inc., Osaka, Japan
Correspondence: Satoshi Obika 1-6 Yamadaoka, Suita, Osaka 565-0871, Japan. E-mail: obika@phs.osaka-u.ac.jp or Mariko Harada-Shiba 5-7-1 Fujishirodai, Suita, Osaka 565-8565, Japan. E-mail: shiba.mariko.ri@mail.ncvc.go.jp
Received 6 November 2011; revised 10 April 2012; accepted 10 April 2012

hepatic PCSK9 mRNA and serum LDL-C. However, a large dose of MOE is necessary to obtain sufficient efficacy. More recently, Gupta *et al.* demonstrated that a reduced amount of 2′,4′-bridged nucleic acid (BNA) (also called as locked nucleic acid (LNA))-modified gapmer efficiently suppresses PCSK9 mRNA and induces an increase in LDLR protein levels both *in vitro* and *in vivo*.[20] Due to the high-affinity binding of 2′,4′-BNA–modified AON molecules, in many cases, 2′,4′-BNA–modified gapmer shows improved antisense potency *in vivo* as compared to MOE-based gapmer. However, in some cases, the repeated administration of 2′,4′-BNA–modified gapmer causes hepatotoxicity.[21] The development of more potent and less toxic antisense molecules is necessary for clinical usage.[22] We have developed a series of 2′,4′-BNAs such as 2′,4′-BNA and 2′,4′-BNA^{NC}, which have chemical bridges between the 2′ and 4′ positions of the ribose rings; 2′,4′-BNA^{NC}–modified oligonucleotides retain high-affinity binding to RNA and higher nuclease stability than 2′,4′-BNA–modified oligonucleotides.[23–25] Therefore, 2′,4′-BNA^{NC}–modified anti-PCSK9 AONs would be expected to possess distinct cholesterol-lowering potency and toxicological risks *in vivo*. Actually, 2′,4′-BNA^{NC}–modified phosphatase and tensin homolog deleted from chromosome ten (PTEN) inhibitor showed high potency without the onset of hepatotoxicity.[26] In this study, we present the effective gene silencing and cholesterol-lowering effects of both 2′,4′-BNA– and 2′,4′-BNA^{NC}–based anti-PCSK9 AON. In addition, we showed the toxicological characteristics of 2′,4′-BNA– and 2′,4′-BNA^{NC}–based AONs.

Results

Physicochemical properties of a 2′,4′-BNA–modified anti-PCSK9 AON *in vitro*

The 2′,4′-BNA–modified phosphorothioate oligonucleotides (P900SL) and a conventional phosphorothioate AON (P900S) were designed based on the previously identified potential sequence.[27] The control sequence was CR01S, which has the same conventional phosphorothioate backbone as P900S, but does not target any specific genes in mice (**Table 1**). Upper and lower case letters in the sequences represent 2′,4′-BNA and DNA, respectively. We additionally selected another sequence, a consensus sequence between the mouse and human sequences to dispense with the sequence translation to adapt to human clinical trials. P901SL and P901SNC both possess five gaps, and nine of 20 nucleotides are substituted by 2′,4′-BNA and 2′,4′-BNA^{NC} (**Table 1**, **Figure 1**). Note that the sequence, length, and composition of AONs have not been fully optimized yet here. The melting temperature (T_m) values of P900S, P900SL, P901S, P901SL, and P901SNC with their target RNA were determined by UV-melting experiments. AONs modified with 2′,4′-BNA and 2′,4′-BNA^{NC} showed an excellent target affinity compared to conventional phosphorothioate AONs (**Table 1**).

In vitro gene silencing properties

We next evaluated *in vitro* gene silencing properties of AONs by using mice hepatic NMuLi cells (**Figure 2a–c**) treated with [Q4] 1–50 nmol/l of P900SL by means of lipofection. Real-time reverse transcription-PCR revealed a dose-dependent reduction of the PCSK9 mRNA level as compared to the GAPDH mRNA level (half-maximal inhibitory concentration (IC_{50}) = 3.0 nmol/l) (**Figure 2a**). By contrast, no such effective reduction of the mRNA level occurred in P900S-treated cells (IC_{50} = 41.2 nmol/l) (**Figure 2a**), and treatment with CR01S and CR01SL did not yield any silencing (**Figure 2b**). To investigate whether suppression of PCSK9 mRNA by P900SL affects the PCSK9 protein level, we performed western blotting experiments. A dose-dependent reduction of the PCSK9 protein level occurred in P900SL-treated NMuLi cells (**Figure 2a**). On the other hand, the protein levels of LDLR in P900SL-treated cells were increased in a dose-dependent manner, showing the inverse relationship between PCSK9 and LDLR protein levels. PCSK9 protein was thoroughly inhibited by P900SL at a concentration of ~10 nmol/l. The increase in LDLR protein simultaneously reached a plateau at this concentration. Gene silencing properties of P901S, P901SL, and P901SNC were demonstrated both in murine and human hepatic cell lines. P901SL and P901SNC showed a similar silencing efficacy as P900SL in NMuLi cells (**Figure 2a**). Both P901SL and P901SNC showed far more efficient mRNA inhibitory activity than P901S in HepG2 cells (**Figure 2d**). The reduction rate of PCSK9 protein levels also supported this trend (**Figure 2e**).

Table 1 Properties of modified oligonucleotides used in this study

Sequence ID	Sequence[a]	T_m	IC_{50} (nmol/l) NMuLi	IC_{50} (nmol/l) HepG2
CR01S	5′-ccttccctgaaggttcctcc-3′	–	N.D.	–
CR01SL	5′-cctTCCctgaagGTTCcTCc-3′	–	N.D.	–
P900S	5′-gggctcatagcacattatcc-3′	37.0	23	–
P900SL	5′-GggCTCatagcaCaTTaTCc-3′	72.1	1.8	–
P901S	5′-ccaggcctatgagggtgccg-3′	49.6	–	100
P901SL	5′-CCaggCCTaTgagggTgCCg-3′	83.2	1.0	1.8
P901SNC	5′-CCaggCCTaTgagggTgCCg-3′	86.0	3.0	11.6

Abbreviations: BNA, bridged nucleic acid; IC_{50}, half-maximal inhibitory concentration.
[a]Oligonucleotides with 2′,4′-BNA (upper case), 2′,4′-BNA^{NC} (capital italic), and DNA (lower case letters). All internucleotide linkages are phosphorothioated. Melting temperature (T_m) of CR01S and CR01SL were not measured because no target site on transcripts, marked "–". Non-detectable IC_{50} values, due to low potency, marked N.D. IC_{50} values were partly not determined, marked "–".

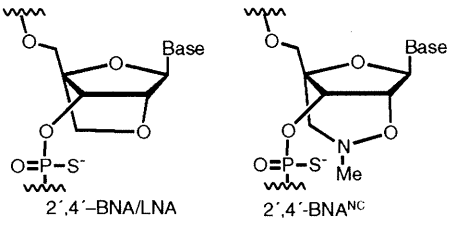

[Q5]

Figure 1 Structure of bridged nucleic acids (BNA) used in this study. LNA, locked nucleic acid.

The level of intrahepatic AONs in normal chow-fed mice after a single treatment with BNA-modified AONs

Next, we examined whether BNA-modified AONs can also be good inhibitors of PCSK9 in mice. A naked AON (P900SL) was intravenously (i.v.), subcutaneously (s.c.), and

intraperitoneally (i.p.) injected into normal chow-fed C57BL/6J mice (**Figure 3**). After 72 hours, the hepatic PCSK9 mRNA [Q7] levels were measured, and the ED_{50} values were determined. Intravenous administration showed the most efficient hepatic reduction of PCSK9 mRNA (ED_{50} = 7.5 mg/kg) (**Figure 3a**). Subcutaneous and intraperitoneal injections resulted in ED_{50} values of 8.8 and 12.1 mg/kg, respectively (**Figure 3c,d**). Next, we measured the amount of intact P900SL that accumulated in the liver after i.v. administration by using a previously described ELISA method.[28] The intrahepatic content of P900SL was directly proportional to the applied doses, and the saturation of accumulation was not observed even at the highest dose of 70 mg/kg, which is consistent with a previous report[29] (**Figure 3b**).

Repeated administration of BNA-modified AONs to atherogenic diet-fed mice

To determine the pharmacological effects of BNA-modified AONs, we monitored the serum cholesterol change upon repeated administration of AONs. Naked AONs (P900S and P900SL) were i.p. injected into atherogenic diet (cholesterol content, 1.25%)-fed C57BL/6J mice twice during 5 days at a dosage of 10 mg/kg per administration. Injections were performed on days 1 and 4. On day 5, livers were harvested to measure gene expression, and blood was collected for the lipid component analysis and toxicity evaluation. As shown in **Figure 4a,** a significant silencing effect of the hepatic PCSK9 mRNA level was only observed in the P900SL-treated arm. The increase in hepatic LDLR protein was shown by western blotting analysis (**Figure 4c**). The average serum LDL-C levels were concomitantly reduced by ~30%, although no statistically significant differences were observed (**Figure 4b**). Collectively, P900SL showed a mild cholesterol-lowering effect in this short-term experiment with the lack of serum elevation of liver transaminases, aspartate aminotransferase and alanine aminotransferase (ALT) (**Figure 4d**).

To obtain cholesterol-lowering efficacy profiles and toxicological information, we next performed longer-term and multiple-dose experiments in mice. P900SL was i.p. injected twice weekly at a dosage of 2–40 mg/kg/week for 6 weeks into high-cholesterol–loaded mice. After 4 weeks of treatment, blood samples were collected from tail veins, and the precise cholesterol profiles in serum lipoproteins were analyzed by the high-performance liquid chromatography method. **Supplementary Table S1** shows the raw serum total cholesterol levels and the cholesterol levels of fractionated lipoprotein components. **Figure 5a,b** show raw data plots of the high-performance liquid chromatography analysis of serum and the serum LDL-C ratio. Total cholesterol levels did not show a cholesterol-lowering effect or any other specific trends with an increase of doses. However, a precise lipoprotein component analysis revealed that P900SL had induced a dose-dependent LDL-C reduction, and the serum LDL-C reduction of 43% was achieved at a dose of 40 mg/kg/week, whereas serum HDL-C levels increased inversely with LDL-C levels. After a 6-week dosing regimen, livers and blood were harvested to analyze gene and protein expression and toxicities. A dose-dependent decrease of LDL-C, as seen at week 4, was continuously observed. Intrahepatic cholesterol content showed no significant difference between arms (**Supplementary Figure S1**). Hepatic gene expression levels were analyzed by the real-time reverse transcription-PCR method. Hepatic PCSK9 mRNA was efficiently reduced in a dose-dependent manner (**Figure 5c**). And, the reduction of PCSK9 mRNA did not affect LDLR mRNA expression levels (**Figure 5e**). However, LDLR protein levels increased concomitantly with decreased LDL-C levels (**Figure 5d**). Hepatic LDLR protein levels were significantly increased by ~1.5-fold in a dose-dependent manner. Note that we here collected sera and analyzed lipid profiles 2 weeks ahead of sacrifice in order to distribute the stressors associated with treatments, which strongly disturbs serum cholesterol levels.

Related gene expression associated with repeated dosing

We further investigated the effect of BNA-modified AONs on molecules related to the cholesterol metabolism (**Figure 5e**). Knockdown of PCSK9 mRNA induced a reduction in the gene expression of sterol regulatory element-binding protein 2 (SREBP2), a transcriptional factor controlling sterol synthesis; hydroxymethylglutaryl-CoA (HMG-CoA) synthase, an enzyme in the cholesterol synthesis pathway; hepatic triglyceride lipase (LIPC); and ATP-binding cassette transporter (ABCA1), a key enzyme for HDL production. On the other hand, scavenger receptor class B type 1 (SR-B1), a receptor for HDL particles, and cholesterol acyltransferase (ACAT1) showed no significant change, and the expression level of cholesterol 7α-hydroxylase (CYP7A1), the first and rate-limiting enzyme in bile acid synthesis, dose-dependently increased.

Toxicological characteristics of BNA-AONs associated with repeated dosing

Toxicological characteristics of P900SL upon subchronic dosing were estimated by an analysis of blood biochemistry and a histopathological analysis (**Figure 6**). Because phosphorothioate AONs accumulate mainly in the kidney and liver,[30–32] hepatotoxicity and renal toxicity are the most likely types of toxicity; 2′,4′-BNA–based AONs have the potential to induce hepatotoxicity.[21] However, our experiments showed only moderate increases in liver transaminases (even at higher doses of P900SL) and a dose-dependent mild increase in serum blood urea nitrogen levels (**Figure 6a**). Histopathologically, no treatment-related changes were seen in the liver or kidneys. As shown in **Figure 6b**, although the majority of mice treated with saline or therapeutic regimes showed cloudy swelling of hepatocytes, no cellular damage was found in the centrilobular and perilobular hepatocytes, which frequently experience toxicological insults. In addition, granulomas or inflammation were sporadically observed in the saline group and treated groups (**Supplementary Table S2**).

Repeated administration of 2′,4′-BNA^{NC}–modified AONs to atherogenic diet-fed mice with the least toxicity

To examine the effect of 2′,4′-BNA^{NC}–modified AONs, P901SNC as well as P901SL were applied to atherogenic diet-fed mice to investigate their potencies and toxicity profiles. P901SL and P901SNC were i.p. administered twice weekly for 6 weeks at a dose of 1–20 and 1–10 mg/kg/injection, respectively. On week 4, peripheral blood was collected from tail

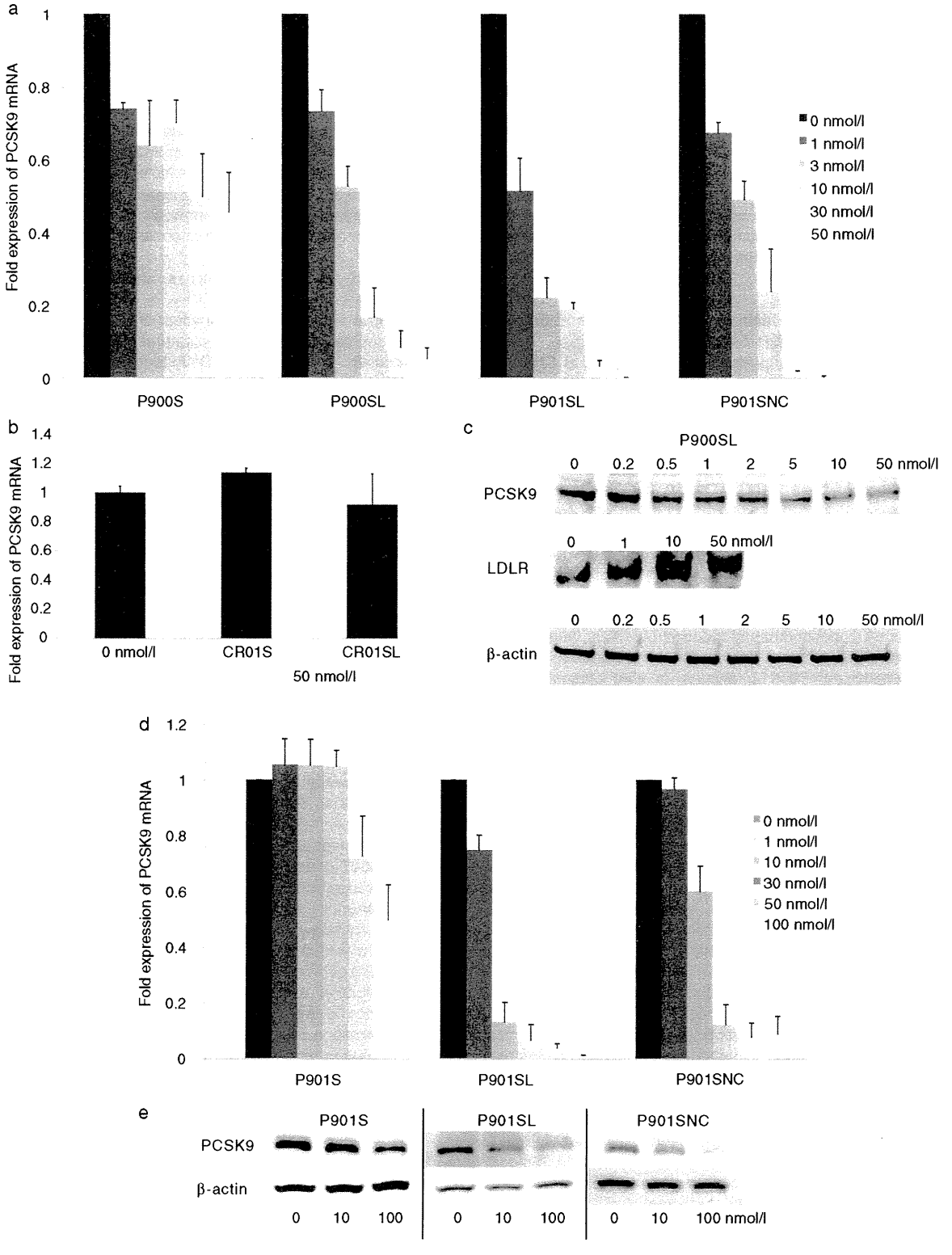
a
Fold expression of PCSK9 mRNA
1
0.8
0.6
0.4
0.2
0
P900S
P900SL
P901SL
P901SNC
0 nmol/l
1 nmol/l
3 nmol/l
10 nmol/l
30 nmol/l
50 nmol/l
b
Fold expression of PCSK9 mRNA
1.4
1.2
1
0.8
0.6
0.4
0.2
0
0 nmol/l
CR01S
CR01SL
50 nmol/l
c
P900SL
0 0.2 0.5 1 2 5 10 50 nmol/l
PCSK9
0 1 10 50 nmol/l
LDLR
0 0.2 0.5 1 2 5 10 50 nmol/l
β-actin
d
Fold expression of PCSK9 mRNA
1.2
1
0.8
0.6
0.4
0.2
0
P901S
P901SL
P901SNC
0 nmol/l
1 nmol/l
10 nmol/l
30 nmol/l
50 nmol/l
100 nmol/l
e
P901S
P901SL
P901SNC
PCSK9
β-actin
0 10 100
0 10 100
0 10 100 nmol/l

veins, and the cholesterol content of each lipoprotein fraction was measured. P901SL showed no significant reduction of LDL-C levels, whereas P901SNC reduced serum LDL-C levels by ~30% at the highest dose (10 mg/kg/injection), and the reduction occurred in a dose-dependent manner (**Figure 7a**). We observed a slower onset of the reduction of LDL-C of P901SL 6 weeks after the first treatment (**Supplementary Figure S2**). Meanwhile, hepatic PCSK9 mRNA expression was suppressed and the hepatic LDLR protein was increased accompanied by AON treatment with relatively large deviations (**Figure 7b,c**). PCSK9 mRNA was inhibited by P901SL and P901SNC as efficiently as P900SL. LDLR protein responded maximally to 20 mg/kg/injection of P901SL and 10 mg/kg/injection of P901SNC. The increasing rates of these two arms were nearly the same (~1.5-fold increase). The lack of severe hepatotoxicities or kidney toxicities was confirmed by serum chemistry in both the P901SL- and P901SNC-treated arms (**Supplementary Table S3**). Collectively, 2′,4′-BNA^{NC}–based AON, P901SNC, was as safe as the 2′,4′-BNA–based counterpart, P901SL.

Discussion

We demonstrated in this article that BNA-based antisense therapeutics successfully inhibited hepatic PCSK9 expression, resulting in a strong reduction of the serum LDL-C levels of mice. Our findings support the hypothesis that PCSK9 is a potential therapeutic target for hypercholesterolemia. To the best of our knowledge, this is the first time that we were able to show that BNA-based AONs induced cholesterol-lowering action in hypercholesterolemic mice. P900SL yielded high inhibitory activity *in vivo* as well as *in vitro*, and i.v. administration gave the highest peak inhibitory activity of the three representative routes. Nevertheless, i.p. and s.c. injections are alternative routes to i.v. injection, because they yielded adequate dose-responsive suppression of PCSK9 mRNA. In fact, Mipomersen for the treatment of hypercholesterolemia is given s.c. rather than i.p. due to practicality.[33,34] The rationality of s.c. injection is also supported by the pharmacokinetic nature and disposition properties of 2′-*O*-methyl phosphorothioate AON.[35] The peak tissue levels of 2′-*O*-methyl phosphorothioate AON after i.v. injection were higher than after s.c. and i.p. administration, and i.v. injection gives the peak of exon skipping efficiency. However, the bioavailability of 2′-*O*-methyl phosphorothioate AON was similar among all routes, and durable effects were observed after s.c. administration; therefore, the investigators selected s.c. administration for a preclinical study in mice. On the other hand, the hepatic accumulation of P900SL associated with a single i.v. injection increased directly with dose. This result was totally consistent with a 2′,4′-BNA gapmer targeting apolipoprotein B.[29] Further research to elucidate the pharmacokinetics of BNA-AONs is now underway.

The *in vivo* silencing properties of 2′,4′-BNA–based AON that targets PCSK9 mRNA were previously reported by Gupta *et al.*[20] They achieved the silencing of PCSK9 concomitantly with the upregulation of hepatic LDLR in female mice. However, they did not mention the cholesterol-lowering effect of the 2′,4′-BNA–based AON. We observed a dose-dependent decrease of LDL-C levels and a dose-dependent increase of HDL-C levels (**Figure 5**). There seems to be no trend in the net changes of serum total cholesterol levels (**Supplementary Table S1**). The increase in LDLR protein levels reported by Gupta *et al.*[20] were a little higher than those in **Figure 5d**. The likely explanation is the difference of experimental conditions in which they have used female NMRI mice with standard maintenance diet, whereas we used male C57BL/6J mice with atherogenic diet which contains 1.25% of cholesterol, 0.5% of cholic acid, and so on. Hepatic influx of these ingredients in the diet are known to strongly induce the downregulation of LDLR and cholesterol biosynthetic enzymes such as HMG-CoA reductase by downregulating SREBPs, important transcriptional factors, which results in LDLR reduction.[13,36,37] We also observed dose-dependent moderate increases of aspartate aminotransferase, ALT, and blood urea nitrogen levels, whereas histopathological analysis revealed no severe hepatic toxicities (**Figure 6**, **Supplementary Table S2**). Collectively, a continuous dosing of P900SL showed potent LDL-C reduction in mice without severe side effects, and this report provides the experimental proof of the cholesterol-lowering effects of BNA-based AONs.

We also achieved a dose-dependent decrease in serum LDL-C levels by using a 2′,4′-BNA^{NC}–based AON (P901SNC) (**Figure 7a**). In this case, serum HDL-C levels and the levels of liver and kidney toxicity indicators were not elevated (**Supplementary Table S3**). When compared with P901SNC, a delayed decrease of LDL-C levels was observed in the P901SL-treated arm (**Supplementary Figure S2**). We also showed here that a 2′,4′-BNA^{NC}–based AON (P901SNC) has greater potential to inhibit PCSK9 and to reduce serum cholesterol levels with no toxicity than a conventional 2′,4′-BNA–based AON. The high-potency and low-toxicity characteristics of a 2′,4′-BNA^{NC}–based AON were previously reported to effectively inhibit PTEN mRNA without elevation of the serum ALT level, whereas elevated serum ALT was observed in the 2′,4′-BNA counterpart-treated arm.[26] Thus, we conclude that 2′,4′-BNA^{NC}–based AONs can be a promising therapeutic agent for antisense therapy. However, the structure-activity relationship of BNA-based AONs still remains to be elucidated.

As previously reported, LDLR mRNA expression was independent of PCSK9 inhibition.[20,27] The coordinate repression of SREBP2, HMG-CoA synthase, and ABCA1 is in agreement with a response to a transient massive influx of cholesterol in the liver (**Figure 5e**). HMG-CoA synthase and ABCA1 are both known to be regulated by SREBP2, whereas SR-B1 and ACAT1 are atypical factors regulated by SREBP2.[3,4]

Figure 2 *In vitro* silencing properties of AONs (CR01S, CR01SL, P900S, P900SL, P901SL, and P901SNC). AONs were transfected into NMuLi cells. (**a**,**b**) After a 24-hour incubation, cells were collected and the expression levels of PCSK9 mRNA were determined. Data represent means ± SD. (**c**) PCSK9 and LDLR proteins were also detected by western blotting. AONs (P901S, P901SL, and P901SNC) were transfected into HepG2 cells. (**d**) After a 24-hour incubation, HepG2 cells were collected and the expression levels of PCSK9 mRNA were determined. Data represent mean values ± SD. (e) PCSK9 and β-actin proteins were detected by western blotting. AON, antisense oligonucleotide; LDLR, low-density lipoprotein receptor; mRNA, messenger RNA.

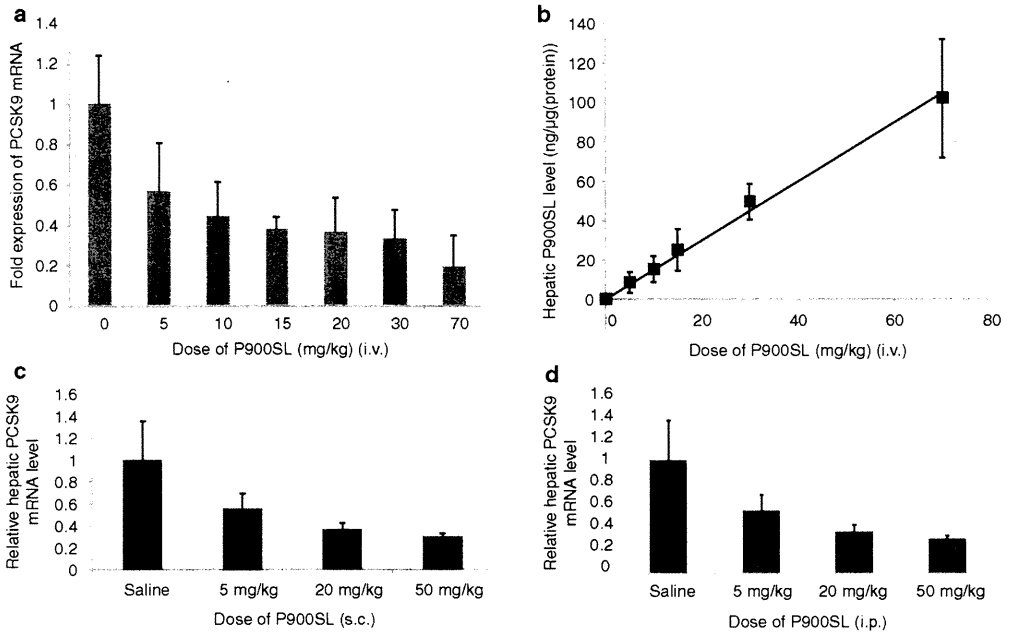

Figure 3 Single administration of P900SL to normal-chow fed C57BL/6J mice. (**a**,**b**) Hepatic PCSK9 messenger RNA (mRNA) level and P900SL content 72 hours after a single intravenous (i.v.) administration were expressed as a function of dose level. (**c**,**d**) Liver PCSK9 mRNA expression level was measured and presented for each dose 72 hours after subcutaneous (s.c.) and intraperitoneal (i.p.) injection, respectively. Data represent mean values ± SD. $n = 4–7$.

The mRNA expression levels of the latter two factors were unchanged by P900SL, while an increased expression level of CYP7A1 was induced by P900SL. CYP7A1 is the first and rate-limiting enzyme in bile acid synthesis; bile acids are versatile signaling molecules that play critical roles in maintaining the homeostasis of cholesterol, lipid, glucose, and energy.[38,39] CYP7A1 deficiency in humans is associated with dyslipidemia, the formation of gallstones, and atherosclerosis.[40] A previous report showed that C57BL/6J mice overexpressing CYP7A1 are less susceptible to atherogenic diet-induced [Q8] elevations of very LDL, IDL, and LDL-C and to reductions of HDL-C and triglyceride and less susceptible to the formation of gallstones and atherosclerosis than their nontransgenic littermates.[41,42] Similarly, under atherogenic conditions, we observed a reduction in the serum LDL-C level and induction of HDL-C in P900SL-treated mice; these effects may be partly due to the induction of CYP7A1 to maintain intrahepatic cholesterol homeostasis. Collectively, we observed the strong induction of CYP7A1 mRNA associated with the strong suppression of PCSK9. Further investigation of underlying mechanisms of PCSK9 inhibition in atherogenic diet-fed mice are necessary to extrapolate the cholesterol-lowering efficacy of PCSK9 inhibitors in humans.

In conclusion, we found that the strong inhibition of PCSK9 by BNA-based AONs can greatly reduce serum LDL-C levels in atherogenic diet-fed mice *via* a novel mechanism of CYP7A1 upregulation. These results indicate that PCSK9 is an excellent drug target for the treatment of hypercholesterolemia. Although a structure of AON has not been fully optimized yet here, the 2′,4′-BNA^{NC}–based AON shows higher potency than its 2′,4′-BNA counterpart and like 2′,4′-BNA shows no toxicity under the conditions tested. Meanwhile, a recent report from Gupta *et al.* demonstrated the superiority of a shorter AON with a smaller number of 2′,4′-BNA modifications over a conventional 20-mer 2′,4′-BNA-gapmer in an antisense potency. They have used a 13-mer AON with five 2′,4′-BNAs and eight gaps that efficiently inhibit the expression of PCSK9 mRNA and protein. We suppose that 2′,4′-BNA^{NC}–based AON also has its own unique optimal structure and a further optimization of sequence, length, and composition of 2′,4′-BNA^{NC}–based AONs would provide a more reliable 2′,4′-BNA^{NC}–based PCSK9 inhibitor.

Materials And Methods

AONs. Two types of modified nucleic acids, 2′,4′-BNA and 2′,4′-BNA^{NC}, were partially incorporated into 20-mer phosphorothioated oligodeoxyribonucleotides with various sequences. CR01S and CR01SL were 20-mer phosphorothioate DNA and 2′,4′-BNA–modified AON, respectively, designed not to target any gene in mice. P900S and P900SL were designed to target murine PCSK9 mRNA, and their sequences have been reported previously. P901S, P901SL, and P901SNC target an identical consensus sequence on mice and human PCSK9 mRNA but have different chemistries. The exact sequences of molecules used in this study are presented in **Table 1**. A large-scale synthesis of 2′,4′-BNA^{NC} units was conducted by BNA. All 2′,4′-BNA^{NC} monomer units were obtained from [Q9] BNA. All modified oligonucleotides were provided by Gene Design (http://www.genedesign.co.jp/). The syntheses were conducted by standard phosphoramidite procedures, and

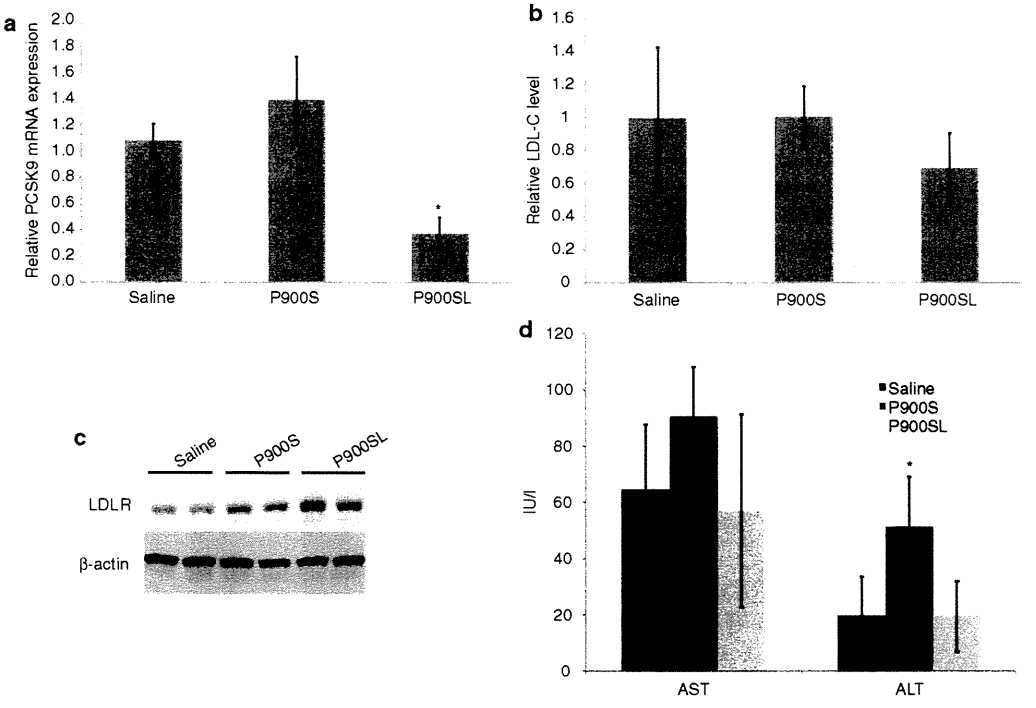

[Q10] **Figure 4 Short-term effects of P900S and P900SL.** Atherogenic diet-fed mice received intraperitoneal administration of P900S or P900SL at a dose of 10 mg/kg twice during 4 days. (**a**) Liver PCSK9 mRNA levels 4 days after the first injection. (**b**) Relative serum LDL-C levels 4 days after the first injection. (**c**) Hepatic LDLR protein expression levels were estimated by western blotting. (**d**) Serum liver transaminases (AST, ALT) were analyzed. Data represent mean values (± SD). $^*P < 0.05$. ALT, alanine aminotransferase; AST, aspartate aminotransferase; LDL-C, low-density lipoprotein cholesterol; LDLR, low-density lipoprotein receptor; mRNA, messenger RNA.

products were carefully processed under aseptic conditions and purified. All products were endotoxin-free and contained low levels of residual salts for *in vivo* usage.

In vitro transfection procedures. For AON transfection experiments, NMuLi cells or HepG2 cells were seeded at 5.0×10^5 cells per well in 6-well plates. AONs were transfected by using [Q11] Lipofectamine 2000 (Invitrogen, Carlsbad, CA) according to the manufacturer's procedures. After a 4-hour transfection, cells were continuously incubated for an additional 20 hours at 37 °C. After incubation, cells were collected and subjected to subsequent analyses.

In vivo pharmacological experiments. All animal procedures were performed in accordance with the guidelines of the Animal Care Ethics Committee of the National Cerebral and Cardiovascular Center Research Institute (Osaka, Japan). All animal studies were approved by an institutional review board. C57BL/6J mice [Q12] were obtained from CLEA Japan. All mice were male, and studies were initiated when animals were 6–8 weeks of age. Mice were maintained on a 12-hour light/dark cycle and fed *ad libitum*. Mice were fed a normal chow (CE-2; CLEA Japan) or an [Q13] artery-hardening food, F2HFD1 (Oriental Yeast, Tokyo, Japan) for 2 weeks before the first treatment and during treatment. Mice received single or multiple treatments of AONs administered i.v, i.p. or s.c. in the dose range of 1–70 mg/kg/injection. Peripheral [Q14] blood was collected from a tail vein in BD Microtainers (BD) for separation of serum. Lipid component analysis of serum was performed by Skylight Biotech (http://www.skylight-biotech.com/). At the time of sacrifice, mice were anesthetized with diethyl ether (Wako). Livers were harvested and snap-frozen [Q15] until subsequent analysis. Whole blood was collected and subjected to serum separation for subsequent analysis.

mRNA quantification. Total RNA was isolated from cultured cells or mouse liver tissues by using TRIzol Reagent (Invitrogen) according to the manufacturer's procedure. Gene expression was evaluated by a two-step quantitative reverse transcription-PCR method. Reverse-transcription of RNA samples was performed by using a High Capacity cDNA Reverse-Transcription Kit (Applied Biosystems, Foster City, CA), and quantitative PCR was performed by a Fast SYBR Green System or TaqMan Gene Expression Assays (Applied [Q16] Biosystems). The mRNA levels of target genes were normalized to the GAPDH mRNA level. The following primer sets were used for quantitative PCRs. Ror murine PCSK9; forward: 5′-TCAGTTCTGCACACCTCCAG-3′, reverse: 5′-GGG TAAGGTGCGGTAAGTCC-3′ and forward: 5′-GCTCAACTG TCAAGGGAAGG-3′, reverse: 5′-CGTTGAGGATGCGGCTA TAC-3′. For human PCSK9; forward: 5′-AAGGGAAGGG CACGGTTAG-3′, reverse: 5′-GAGTAGAGGCAGGCATCG TC-3′. For murine GAPDH; forward: 5′-GTGTGAACGGATTT GGCCGT-3′, reverse: 5′-GACAAGCTTCCCATTCTCGG-3′

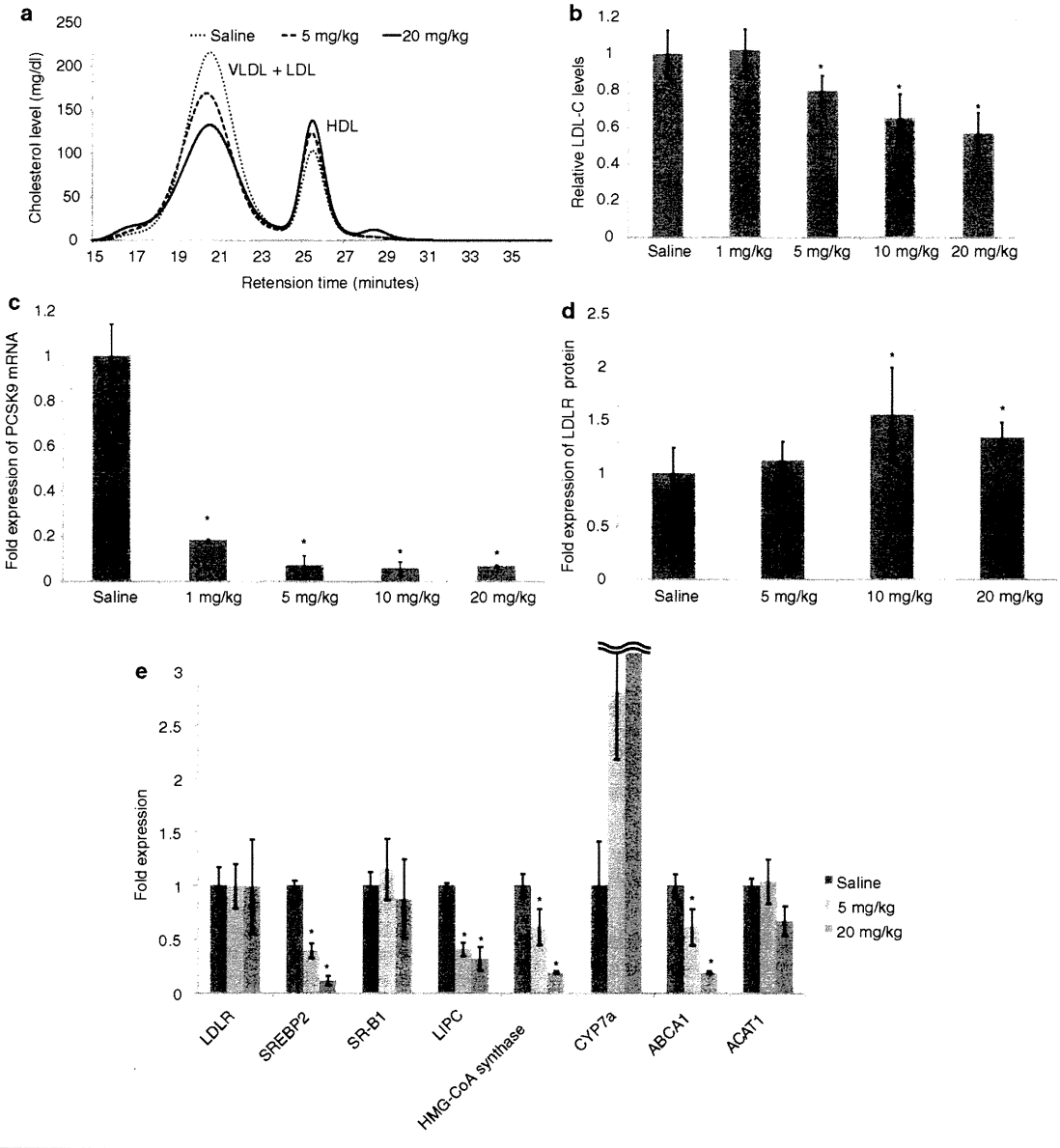

Figure 5 Dose-dependent responses of physiological parameters to P900SL dosing. (**a**) Changes in cholesterol fractions upon administration of P900SL analyzed by HPLC. (**b**) Ratio of serum LDL-C levels after 4 weeks of treatment to before treatment were arranged in order of doses. (**c**) Liver PCSK9 mRNA levels were measured at all dose levels after 6 weeks of treatment. (**d**) Hepatic LDLR protein levels were determined 6 weeks after treatment started. (**e**) The expression levels of genes regulating lipid homeostasis in liver were analyzed. Data represent mean values ± SD. $^*P < 0.05$. $n = 5$. HDL, high-density lipoprotein; HPLC, high performance liquid chromatography; LDL, low-density lipoprotein; LDL-C, LDL cholesterol; LDLR, LDL receptor; mRNA, messenger RNA; VLDL, very LDL.

[Q17] and for human GAPDH; forward: 5′-GAGTCAACGG ATTTGGTCGT-3′, reverse: 5′-GACAAGCTTCCCGTTCTC AG-3′. For murine LDLR, SREBP2, SR-BI, LIPC, HMGCS2, CYP7A1, ABCA1, and ACAT1, TaqMan Gene Expression Assays were used; assay IDs: Mm00440169_ m1, Mm01306297_g1, Mm00450236_m1, Mm01147313_m1, Mm00550050_m1, Mm00484152_m1, Mm01350760_m1, Mm00507463_m1, respectively.

Western blotting analysis. Cultured cells and frozen liver tissues were suspended in lysis buffer (150 mmol/l NaCl, 1.0% IGEPAL CA-630, 0.5% sodium deoxycholate, 0.1% SDS, 50 mmol/l Tris, pH 8.0, 20 × Complete Mini protease inhibitor cocktail 1:20 (Roche, Indianapolis, IN)) and homogenized with [Q18] TissueLyser II (Qiagen, Valencia, CA). Total protein concen- [Q19] trations were measured with a detergent compatible assay kit (Bio-Rad). Solutions were subjected to electrophoresis on 16 [Q20]

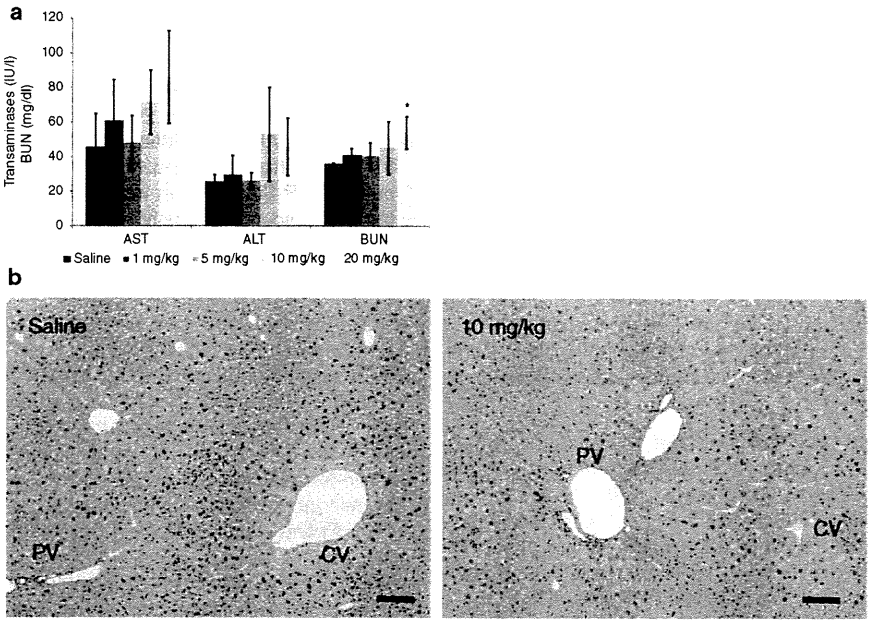

Figure 6 Changes in toxicological parameters upon P900SL dosing. (**a**) Serum liver transaminases (AST and ALT) and BUN levels were measured. Data represent mean values ± SD. $^{*}P < 0.05$. (**b**) Representative H&E stain images of liver of saline- and P900SL-treated mice. Bar indicates 100 µm. AST, aspartate aminotransferase; ALT, alanine aminotransferase; BUN, blood urea nitrogen; CV, central vein; H&E, hematoxylin and eosin; PV, portal vein.

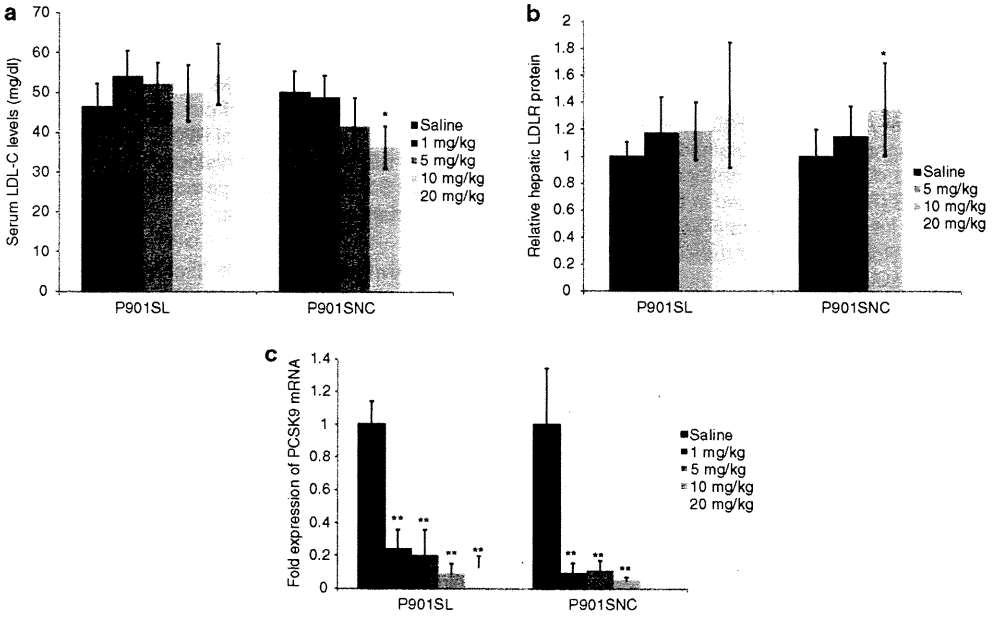

Figure 7 Dose-dependent and chemistry-dependent differences in serum LDL-C levels, hepatic LDLR protein, and PCSK9 mRNA levels after treatment of P901SL and P901SL. (**a**) Raw values of serum LDL-C were obtained at 4th week of schedule. (**b**) Hepatic LDLR protein expression levels were measured after the end of the schedule. (**c**) Liver PCSK9 mRNA levels were measured at all dose levels after 6 weeks of treatment. Data represent mean values ± SD. $^{*}P < 0.05$, $^{**}P < 0.001$ (versus a saline-treated control arm). $n = 5$. LDL-C, low-density lipoprotein cholesterol; LDLR, low-density lipoprotein receptor; mRNA, messenger RNA.

or 6% Tris-glycine gels (Invitrogen) and transferred to a polyvinylidene difluoride membrane (Bio-Rad). PCSK9 western blotting was performed at room temperature for 1 hour with [Q21] a primary anti-rabbit PCSK9 antibody (1:200; Abcam). Additional analyses were performed by using anti-LDLR antibody [Q22] (R&D Systems, Minneapolis, MN) and anti-β actin antibody [Q23] (Cell Signaling). Membranes were washed three times with phosphate-buffered saline containing 0.3% Tween 20. Blots were labeled by using horseradish peroxidase-conjugated secondary antibodies, either goat anti-rabbit or donkey anti- [Q24] goat antibodies (Santa Cruz Biotechnology, Santa Cruz, CA). Chemiluminescent detection was performed by using an ECL [Q25] plus Western blot detection kit (Amersham Biosciences), and bands were visualized by using an LAS-4000mini image ana- [Q26] lyzer (Fuji Film). β-Actin expression levels were used as an internal standard.

The determination of P900SL content in liver

Materials and reagents. The template DNA was a 29-mer DNA (5′-gaatagcgaggataatgtgctatgagccc-3′), which is complementary to P900SL, with biotin at the 3′-end. The ligation probe DNA was a 9-mer DNA (5′-tcgctattc-3′) with phosphate at the 5′-end and digoxigenin at the 3′-end. The template DNA and the ligation probe DNA were purchased from Japan [Q27] Bio Service. Reacti-Bind NeutrAvidin-coated polystyrene [Q28] strip plates were purchased from Thermo Fisher Scientific (nunc immobilizer streptavdin F96 white, 436015). The template DNA solution (100 nmol/l) was prepared in hybridization buffer containing 60 mmol/l Na_2HPO_4 (pH 7.4), 0.9 mol/l NaCl, and 0.24% Tween 20. The ligation probe DNA solution (200 nmol/l) was prepared in 1.5 units/well of T4 DNA ligase [Q29] (TaKaRah) with 66 mmol/l Tris-HCl (pH 7.6), 6.6 mmol/l $MgCl_2$, 10 mmol/l DTT, and 0.1 mmol/l ATP.

The washing buffer used throughout the assay contained 25 mmol/l Tris-HCl (pH 7.2), 0.15 mol/l NaCl, and 0.1% Tween 20. Anti-digoxigenin-AP antibody (Fab fragments conjugated with alkaline phosphatase) was obtained from Roche Diagnostics. A 1:2,000 dilution of the antibody with 1:10 super [Q30] block buffer in TBS (Pierce) was used in the assay. The alkaline phosphatase luminous substrate was prepared in 250 μmol/l CDP-Star (Roche) with 100 mmol/l Tris-HCl (pH 7.6) and 100 mmol/l NaCl.

Sample preparation. Frozen liver tissue was collected in a 2-ml tube with 1 ml of phosphate-buffered saline and a [Q31] zirconia ball (ø 5 mm, Irie) and mechanically homogenized for 2 minutes at 30 oscillations per second by a TissueLyser II apparatus (Qiagen). Total protein concentrations were measured with a detergent compatible assay kit (Bio-Rad) and adjusted to 8 mg/l with phosphate-buffered saline. The assay was performed at the concentration range of 128 pmol/l–400 nmol/l in duplicate. For the standard curve, 10 standard solutions were prepared. To AON-untreated mice, liver [Q32] homogenates were added to P900SL solutions to prepare 10 standard samples at a range of 128 pmol/l–400 nmol/l.

Assay procedures. The template DNA solution (100 μl) and standard solution (10 μl) or liver homogenates (10 μl) containing the P900SL were added to Reacti-Bind Neutr Avidin-coated polystyrene strip 96-well plates and incubated at 37 °C for 1 hour to allow the binding of biotin to streptavidin-coated wells and hybridization. After hybridization, the plate was washed three times with 200 μl of washing buffer. Then, ligation probe DNA solution (100 μl) was added, and the plate was incubated at room temperature (15 °C) for 3 hours. The plate was then washed three times with the washing buffer. Subsequently, 200 μl of a 1:2,000 dilution of anti-digoxigenin-AP was added, and the plate was incubated at 37 °C for 1 hour. After washing three times with the washing buffer, CDP-Star solution was added to the plate, and finally the luminescence intensity was determined by using a Centro XS^3 luminometer (Berthold) one second after the addition [Q33] of CDP-Star. The linear range of 128 pmol/l–400 nmol/l in this ELISA system was determined as $r > 0.99$.

Serum chemistry and hematoxylin and eosin staining. Serum from blood collected from the inferior vena cava upon sacrifice was subjected to serum chemistry. Assay kits (WAKO) were used to measure serum levels of aspartate aminotransferase, ALT, blood urea nitrogen, and creatinine, which are biomarkers for hepatic and kidney toxicities. Formalin-fixed liver samples (20% formalin; WAKO) were sliced by microtome (Leica Microsystems), embedded in Histsec [Q34] (Merck) and stained with Carrazzi's hematoxylin and Tissue- [Q35] Tek eosin solutions.

Statistical analysis. Pharmacological studies were performed with 5–7 mice per treatment group. A Student's *t*-test was performed for comparison of two arms. $P < 0.05$ or $P < 0.01$ was considered to be of statistical significance.

Supplementary Material

Figure S1. Comparison of intrahepatic cholesterol levels between control and 20 mg/kg/injection of P900SL-treated arms.
Figure S2. Relation between given dose and serum LDL-C levels of P901SL 6 weeks after treatment started.
Table S1. Serum raw cholesterol levels in atherogenic diet-fed mice after 4 weeks of P900SL treatment.
Table S2. Summary of histopathological findings.
Table S3. Toxicological parameters.
Materials and Methods. [Q36]

Acknowledgments. We thank E. Shibata, M. Inoue, M. [Q37] Morimoto, and M. Sone for their technical support, who are affiliated with National Cerebral and Cardiovascular Center Research Institute. A part of this work was supported by the Program for Promotion of Fundamental Studies in Health Sciences of the National Institute of Biomedical Innovation (NIBIO) and a research grant from the Ministry of Health, Labor, and Welfare (H23-seisakutansaku-ippan-004). T.Y. thanks the Research Fellowship from the Japan Society for the Promotion of Science (JSPS) for Young Scientists. T.I. is a CEO of BNA Inc., the company that produces 2′,4′-BNA^{NC} monomers. The other authors declared no conflict of interest. [Q38]

1. Jones, P, Kafonek, S, Laurora, I and Hunninghake, D (1998). Comparative dose efficacy study of atorvastatin versus simvastatin, pravastatin, lovastatin, and fluvastatin in patients with hypercholesterolemia (the CURVES study). *Am J Cardiol* **81**: 582–587.
2. Goldstein, JL and Brown, MS (2009). The LDL receptor. *Arterioscler Thromb Vasc Biol* **29**: 431–438.
3. Horton, JD, Goldstein, JL and Brown, MS (2002). SREBPs: activators of the complete program of cholesterol and fatty acid synthesis in the liver. *J Clin Invest* **109**: 1125–1131.